

HYDRAULIC ASSESSMENT OF TRADITIONAL AND FISH-FRIENDLY TIDE
GATES IN HUMBOLDT BAY, CALIFORNIA

By

Marcela Anne Jimenez

A Thesis Presented to

The Faculty of Humboldt State University

In Partial Fulfillment of the Requirements for the Degree

Master of Science in Environmental Systems: Environmental Resources Engineering

Committee Membership

Dr. Margaret Lang, Committee Chair

Dr. Eileen Cashman, Committee Member

Antonio Llanos, Committee Member

Dr. Margaret Lang, Program Graduate Coordinator

July 2021

ABSTRACT

HYDRAULIC ASSESSMENT OF TRADITIONAL AND MUTED, FISH-FRIENDLY TIDE GATES IN HUMBOLDT BAY, CALIFORNIA

Marcela Anne Jimenez

Tide gates are common hydraulic structures located throughout coastal and estuarine areas that prevent tidal waves from flooding previously converted tidally influenced areas. As restoration efforts increase, more “fish-friendly” tide gates that allow for larger openings and longer opening periods are being installed to improve habitat for threatened or endangered species. The purpose of this thesis was to determine discharge and head loss coefficients for traditional and side-hinged tide gates that could be inputs for hydraulic models and improve tide gate sizing and design. The study sites included Gannon Slough and US 101 Slough in Humboldt, California that represented a traditional, top-hinged gate and a side-hinged gate, respectively. Discharge, water levels and angle measurements of the gates were all collected during gate openings. These values were used to determine discharge coefficients for Gannon Slough, head loss coefficients for US 101 Slough, and analyze fish passage through each site. At Gannon Slough, discharge coefficients ranged between 0.12 and 0.86. US 101 Slough’s head loss coefficients ranged between 1.09 and 16.07. Both hydraulic parameters were compared to angle opening and discharge in attempt to identify patterns that could be related to different phases throughout the opening. However, the parameters did not produce

distinguishable values related to the openings. Future recommendations include increasing measurements during gate measurements and an exploration at various flow events.

ACKNOWLEDGEMENTS

First off, I would like to thank my thesis advisor, Professor Margaret Lang. Each of your classes inspired me during undergrad and it was an honor being able to work with you on multiple projects throughout my graduate career. Thank you for all your patience and sorting through the data with me.

I would like to thank Professor Eileen Cashman and Tony Llanos, P.E., for being part of my committee. Eileen, you brought a fresh pair of eyes to my project. Tony, you were integral in helping me get acquainted with tide gate monitoring and always had great idea to improve the project throughout the whole process.

Thank you to Mike Love, P.E. and Thomas Gast for all the guidance during data collecting and processing.

Thank you to Caltrans for allowing me to be a part of the larger Tide Gate Monitoring Project and providing funding for data collection.

I would also like to thank Alyssa Virgil, Tyler Caseltine, Chris Fabbri and David Rivera for all their help with field work and data processing. It was a pleasure trekking through the muck with each of you.

And finally, I would like to thank my family and friends for all the support you have provided throughout my time in school.

TABLE OF CONTENTS

ABSTRACT.....	ii
ACKNOWLEDGEMENTS	i
TABLE OF CONTENTS.....	ii
LIST OF TABLES	v
LIST OF FIGURES	vi
LIST OF APPENDICES	ix
INTRODUCTION	1
LITERATURE REVIEW	4
History and Use of Tide Gates.....	4
Hydraulics in an Estuarine Setting.....	5
Types of Tide Gates	5
Effects of Tide Gates on Ecology and Habitat	11
Gate Design Criteria	15
General Tide Gate Design.....	15
Tide Gate Passage Requirements	17
Tide Gate Hydraulic Analysis.....	21
Total Head Loss	21
Energy Loss Coefficients	23
Simulating Tide Gates in Hydrodynamic Models	27
MATERIALS AND METHODS.....	40
Study Sites	40

Data Collection	43
Daily Monitoring	43
Velocity and Discharge Measurements.....	47
Data Processing.....	54
Velocity Analysis.....	54
Energy Loss Analysis	57
Total Head Loss	58
Entrance Head Loss	59
Friction Head Loss	60
Tide Gate/Exit Head Loss	61
Discharge Coefficient	62
RESULTS	64
Gannon Slough	64
US 101 Slough.....	70
Discharge Coefficient	76
Fish Passage.....	78
DISCUSSION	81
Gannon Slough	81
US 101 Slough.....	83
Discharge Coefficient Discussion.....	85
Fish Passage Criteria.....	86
RECOMMENDATIONS AND CONCLUSIONS	88
Recommendations.....	88

Gannon Slough.....	88
US 101 Slough	89
Conclusions.....	90
REFERENCES	93
APPENDICES	96

LIST OF TABLES

Table 1. Percent time water temperatures were within various growth boundaries for juvenile Chinook salmon. Table adopted from Tonnes (2006).	12
Table 2. High design flow criteria for fish passage in culverts for salmonid and non-salmonid species set by the California Department of Fish and Wildlife. Table adapted from (CDFG 2004).	18
Table 3. Low design flow criteria for fish passage in culverts for salmonid and non-salmonid species set by the California Department of Fish and Wildlife. Table adapted from (CDFG 2004).	18
Table 4. Maximum velocity and minimum depth criteria for fish passage in culverts for salmonid set by the California Department of Fish and Wildlife. Table adopted from (CDFG 2004).	18
Table 5. Maximum velocity criteria for fish passage in culverts for adult salmonid set by the California Department of Fish and Wildlife. Table adopted from (CDFG 2004).	19
Table 6. Percent time passable for upstream and downstream movement based on juvenile salmon and steelhead design low and high flows. Table adopted from Love et al. (2013).	31
Table 7. Percent time passable for upstream and downstream movement based on adult salmon and steelhead design low and high flows. Table adopted from Love et al. (2013).	31
Table 8. Data loggers used to monitor water level, conductivity and dissolved oxygen. Data Loggers were manufactured by Onset.	45
Table 9. Summary of basic statistics regarding the discharge coefficient of each gate at Gannon Slough.	70
Table 10. Statistics of tide gate head loss values for Gate 1 and Gate 2 at US 101 Slough. Values were based on measurements taken in the field on June 10th, 2020.	75
Table 11. Tide gate coefficient values for US 101 Slough Gate 1. Angle range was based only on angles measured by hand.	76
Table 12. Tide gate coefficient values for US 101 Slough Gate 2. Angle range was based only on angles measured by hand. Gate 2 closed almost instantaneously, preventing any measurement during the Gate Closing phase.	76

LIST OF FIGURES

Figure 1. Basic design concept for a tide gate system. Figure adopted from (Giannico and Souder 2005).	6
Figure 2. A traditional tide gate design demonstrating how the upstream and downstream head differential opens and closes the gate.	7
Figure 3. A side-hinged tide gate design demonstrating how the upstream and downstream head differential opens and closes the gate.	9
Figure 4. Diagrams of an a) permanent opening, b) aside-hinged pet door, c) a top-hinged tide gate and d) a bottom-hinged tide gate.	10
Figure 5. Connectivity results from Greene et al. (2012) showing time (hours) versus surface elevation (meters). Shaded areas represent when gates were closed. Results for the flap gate and the SRT show water surface elevation downstream (thin line) and upstream (bold line) the tide gates. Figure adopted from Greene et al. (2012).	14
Figure 6. Energy grade line showing the decline through the culvert and gate. Figure shows losses due to the culvert entrance, friction losses and outlet losses. Outlet losses comprise of culvert outlet and tide gate losses.	22
Figure 7. Head loss versus flow results for the SCS calculated head loss for pin-hinged gates and laboratory tested rubber flexure (elastic) hinges. Adopted from Replogle and Wahlin (2003).	25
Figure 8. Head loss relative to velocity head versus angle of gate opening for laboratory tested rubber flexure (elastic) hinges with various gate weights. Adopted from Replogle and Wahlin (2003).	27
Figure 9. Discharge coefficient versus downstream (h_d) over upstream (h_u) water depth ratio for the shallow water (SW) model and experimental results. Type A results are on the left and Type B results are on the right. B/h_u refers to ratio of the cross-sectional width to the channel depth. Theta refers to the angle of the gate opening. Figure adopted from Cassan et al. (2018).	35
Figure 10. Complete and quasi-steady solutions for flow and gate opening for different stiffener constants. Figure shows two plots with the first (left) showing time versus flow and the second (right) showing time versus theta. Figure adopted from Guiot et al. (2020).	38
Figure 11. Image of the Gannon Slough gates and the downstream (tidal) channel.	41

Figure 12. Image of one of the US 101 Slough gates while it is open. Image taken downstream of the gate. Photo taken by Antonio Llanos.	42
Figure 13. Image of a field crew member downloading loggers next to the stand-pipes holding water level, salinity and DO loggers at Gannon Slough Station 4.	44
Figure 14. Gannon Slough monitoring stations used for daily monitoring between May 2019 and June 2020. All stations measured water level, salinity, and temperature. Stations 3 and 4 also included dissolved oxygen loggers.	46
Figure 15. US 101 Slough monitoring stations used for daily monitoring between May 2019 and June 2020. All stations measured water level, salinity, and temperature. Station 4 also included a dissolved oxygen logger.	47
Figure 16. Image showing how the discharge measurements were taken using the ADCP at Gannon Slough along the upstream cross-section. Additional image showing the ADCP on the rigid trimaran.	49
Figure 17. Gannon Slough monitoring stations used during angle and ADCP measurements performed on May 18, 2020. Stations 1 and 2 are the permanent data collection stations. Stations 1.25 and 1.75 are temporary stations installed during ADCP measurements.	51
Figure 18. US 101 Slough monitoring stations used during angle and ADCP measurements performed on June 10, 2020. Stations 1 and 2 are the permanent data collection stations. Stations 1.25 and 1.75 are temporary stations installed during ADCP measurements.	52
Figure 19. Diagrams comparing the normal monitoring setup compared additional measurements collected during the 2020 ADCP measurement setups at Gannon and US 101 Slough. (a) shows the general monitoring setup used at both locations. Each station has a water level logger, a bottom salinity logger and a surface salinity logger. (b) shows the Gannon Slough setup used on May 18, 2020. The green stations had 1-minute interval loggers and were used for the head loss analysis. The station within the culvert (STA 1.25) is a water level logger. (c) shows the US 101 Slough setup used on June 10, 2020. The green station had 1-minute interval loggers and were used for the head loss analysis. The station within the culvert (STA 1.75) is a water level logger.	53
Figure 20. Diagram of profile for top hinged gate at Gannon Slough showing what is considered the opening area. The bottom area is calculated by multiplying w by the width of the culvert.	55
Figure 21. Plan view diagram of side hinged gate at US 101 Slough showing what is considered the opening area.	56

Figure 22. Culvert configurations from Jones et al. (2006). US 101 Slough used Culvert A's entrance loss coefficient and Gannon Slough used Culvert B's entrance loss coefficient. Figures adopted from Jones et al. (2006).....	60
Figure 23. Plot showing discharge versus time entering each culvert at Gannon Slough during ADCP measurements taken on May 18, 2020.....	66
Figure 24. Discharge coefficient versus discharge for Gannon Slough measurements taken on May 18, 2020. Gate 1 and Gate 2 had discharge coefficients greater than 1 that occurred when the angle opening was below 0.5 degrees. Outliers are not shown.	68
Figure 25. Discharge coefficient versus gate angle opening for Gannon Slough measurements taken on May 18, 2020. Gate 1 and Gate 2 had discharge coefficients greater than 1 that occurred when the angle opening was below 0.5 degrees. Outliers are not shown.	69
Figure 26. Average velocity through the gate openings and total discharge for US 101 Slough. Velocity measurements correspond to when in-field angle measurements were taken.	72
Figure 27. Total head loss and head loss components at US 101 Slough's Gate 1 based on measurements performed on June 10th, 2020. Head loss comprised of entrance loss, trash rack loss, friction loss and gate loss.....	73
Figure 28. Total head loss and head loss components at US 101 Slough's Gate 2 based on measurements taken on June 10th, 2020. Head loss comprised of entrance loss, trash rack loss, friction loss and gate loss.....	74
Figure 29. Water depth ratio versus tide gate discharge coefficient results from Cassan et al. (2018) and US 101 Slough that was calculated using the same method as Cassan et al. (2018). Figure adapted from Cassan et al. (2018).	77
Figure 30. Average velocities through each Gannon Slough gate compared to fish passage velocity criteria for juvenile and adult salmonids (CDFG 2004).	79
Figure 31. Average velocities through the US 101 Slough tide gates compared to the fish passage velocity criteria for juvenile and adult salmonids (CDFG 2004).	80

LIST OF APPENDICES

Appendix A: Raw ADCP Discharge, Velocity and Angle Measurements	96
Appendix B: Component Head Loss and Discharge Coefficient Calculations for Gannon Slough	100
Appendix C: Component Head Loss Calculations for US 101 Slough	102

INTRODUCTION

Tide gates are common structures in coastal and estuarine settings that prevent upland flooding of converted tidal lands. They often create a barrier to fish and alter the natural brackish environment. Many traditional gates are being replaced with fish-friendly gates meant to allow for better passage of aquatic organisms and improved habitat. Proper tide gate design, including understanding the hydraulics, is needed to properly replace tide gates and improve passage, water quality and increase the reach of brackish habitat. Small-scale tide gate hydraulic performance has not been well characterized for either traditional or fish-friendly gates.

The purpose of this thesis is to determine hydraulic parameters, including head loss and discharge coefficients, for traditional and fish-friendly gate. These values are commonly used in hydraulic models and can improve tide gate design. Additionally, by quantifying these values, variations throughout the opening can be identified to increase the accuracy of the models.

The estuarine conditions along Humboldt Bay provide habitat for plants and anadromous species. Native tidal plants along Humboldt Bay include eelgrass (*Zostera*), Humboldt Bay owl's clover (*Castilleja ambigua* ssp. *Humboldtiensis*), Point Reyes bird's-beak (*Chloropyron maritimum* ssp. *palustre*) and the Humboldt gumplant (*Grindelia stricta* ssp. *blakei*) (USFWS 2013a). Tide gates can negatively impact these plants due to the lack of saltwater entering above the tide gate and decreasing the brackish environment they need to survive (Giannico and Souder 2005).

Anadromous salmonids and the tidewater goby (*Eucyclogobius newberryi*) are the main species of interest for this project. Anadromous salmonids that have been present in the Humboldt Bay are coho salmon (*Onchorhynchus kisutch*), steelhead trout (*Onchorhynchus mykiss*) and chinook salmon (*Onchorhynchus tshawytscha*) (USFWS 2013b). Each of these species are migratory and spend a portion of their adulthood in saltwater. The transition from freshwater to saltwater requires smoltification, or acclimation in brackish water of juvenile salmonids prior to moving to the ocean. Depending on the tributary and salmonid species, the estuarine habitat needs vary because salinity concentrations and concentration gradients will vary from stream to stream. Additionally, salmonids can be present at various depths in the water column depending on the degree of mixing and the vertical salinity and temperature gradients (Moyle et al. 2017).

The tidewater goby is an endangered species that is found along Southern Oregon and the California Coast. They are mainly present in brackish waters and are most commonly found where salinity is less than 12 ppt (USFWS 2005).

The hydraulic performance of traditional and muted fish-friendly gates at two tide gate sites along Humboldt Bay is characterized in this thesis. Gannon Slough and US 101 Slough are both habitat for salmonids and tidewater goby (USFWS 2013b). The Gannon Slough tide gate consisted of three top-hinged gates originally installed in 1954. This site had limited passage due to its traditional gate design and the gates' deteriorating condition. The gates were replaced in September 2020. US 101 Slough has two fish-friendly, side-hinged tide gates to aide in fish passage and allow salt water to enter

upstream of the gate and maintain eel grass habitat. The US 101 Slough gates were installed in January 2019.

Discharge, velocity, and gate angle opening were measured at both sites to calculate hydraulic parameters for each gate during complete gate opening cycles. The calculated coefficients were compared to determine how they vary throughout the gate opening and to identify parameter values that would be most appropriate for hydraulic models of similar small-scale tide gate systems.

LITERATURE REVIEW

The following section discusses relevant information related to hydraulic performance and fish passage criteria for small-scale tide gates. This section begins by describing what tide gates are and how they are used. This is followed by different tide gate types and a general description of how they are designed. The final section highlights previous tide gate hydraulic analyses.

History and Use of Tide Gates

Tide gates are hydraulic structures commonly installed in coastal and estuarine settings to prevent flooding, saltwater intrusion or erosion of converted marshlands. Tide gates, or similar hydraulic structures, have been used for centuries to regulate the flow of water. Wetland conversion in the western United States began in the 1860s as wetlands and estuarine areas were converted for agriculture use (Dahl and Allord 1997). Wetland conversion, mainly for agriculture, has resulted in a 91 percent loss of California's wetlands (USGS 1997). Humboldt Bay's marshland has been reduced by 86 percent since the late 1800s with the majority of the land converted to agricultural (USFWS 2013a).

Conversion of marshland usually consists of building up levees and installing flow control devices (such as tide gates) along channels to prevent tidal incursion and upstream flooding. Tide gates and other hydraulic structures can alter the local habitat and result in negative physical and biological impacts. Tide gates can lead to physical changes to the channel including upstream sedimentation, erosion, or scour. Reduced

mixing, or tidal exchange, may result in abrupt temperature differences and changes in the concentrations and salinity gradient in tidally influenced upstream channels. Tide gates also limit passage or passage times for anadromous and tidal fish species due to long periods of closure (Giannico and Souder 2005). According to the Passage Assessment Database maintained by the California Department of Fish and Wildlife, there are 86 tide gate structures within Humboldt County, with 22 identified as a total barrier for anadromous fish (CDFW 2020).

Hydraulics in an Estuarine Setting

Hydraulics of an estuarine stream differ from upstream fresh-water streams due to the tidal influence. Higher tides result in a larger volume of saltwater entering upstream and lower tides result in less saltwater. Without any control structure in place, estuary channels have varied hydraulic conditions depending on the tide level. Tidal influences can affect the range and concentration of salinity, as well as flow direction, velocities during ebb and flood tides, and sediment transport.

Types of Tide Gates

The basic design of a tide gate system involves a culvert placed within a dike that has a gate placed on the downstream side (Figure 1). The gate closes as tidal elevation increases to prevent tidal water from flooding land upstream of the gate and dike during high tides and allows the upstream land to drain during low tides (Giannico and Souder 2005).

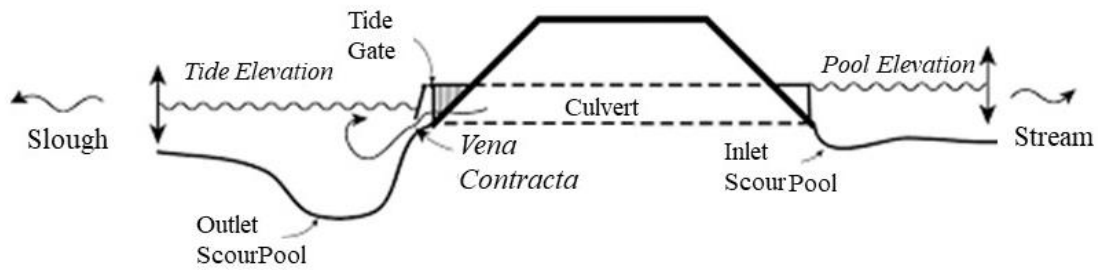


Figure 1. Basic design concept for a tide gate system. Figure adopted from (Giannico and Souder 2005).

Multiple tide gate designs exist to prevent upstream flooding. The following section summarizes traditional and new tide gate designs popular along the US West Coast. The list includes current and potential tide gate designs for Humboldt Bay.

Top-Hinged Tide Gates

Top-hinged tide gates, also referred to as flap gates, are considered traditional tide-gates that do not allow for adequate fish passage. Prior to restoration projects and initiatives, these were common gate types made of either wood or metal. The weight of the gate material and its top-hinged configuration require a large head differential between the upstream and downstream sides of the gate for the gate to open (Figure 2). The large head differential requirement results in a passage barrier. The gates rarely open, especially in drier time periods when there is little fresh water upstream. Additionally, the gates open only a few degrees, forcing large flows through a small area and result in high velocities that are above fish passage criteria and geomorphic changes along the channel (Giannico and Souder 2005).

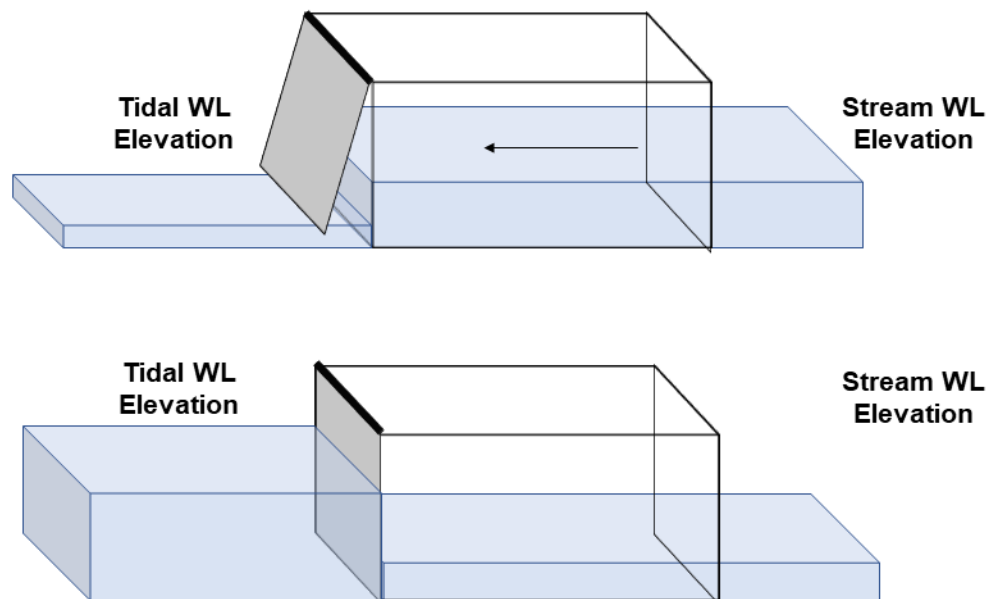


Figure 2. A traditional tide gate design demonstrating how the upstream and downstream head differential opens and closes the gate.

Traditional, top-hinged tide gates also alter habitat through physical changes to the surrounding stream and water quality. Scour pools are common upstream and downstream of the culvert. This is due to water being restricted from flowing downstream when the gate is closed and a jet occurring through the gate when they are open. Additionally, the decrease in tidal and freshwater exchange can result in sedimentation occurring upstream. Traditional tide gates are particularly good at blocking salt water from entering the channel upstream of the tide gates since they are usually closed. This can lead to a reduction in tidal habitat because brackish water cannot extend as far upstream as it naturally would. When a gate leaks and salt water does make it upstream

of the tide gate, mixing still does not occur since the channel is blocked and velocities are not high enough to mix the fresh and salt water (Giannico and Souder 2005).

Side-Hinged Tide Gates

Present day side-hinged gates are made of stainless steel and aluminum and require a smaller head differential to open the gate compared to top-hinged gates. Side-hinged gates are set at an angle along the hinge and allow the gate to remain closed until the upstream pressure is large enough to open the gate (Figure 3) (Giannico and Souder 2005). It is assumed that side-hinged gates require a smaller head differential to open because the water pressure does not need to support the gate weight and allows for better fish passage. This allows them to remain open longer and open to a larger extent than top-hinged gates. The flow exiting an open side-hinged gate passes through a larger cross section area which results in lower velocities that more likely provide fish passage. However, there have been minimal studies that confirm the passage efficiency differences between these two gate designs (CTC & Associates 2016).

Similar to top-hinged gates, side-hinged gates can also affect water quality. Side-hinged gates do not allow for mixing between freshwater and salt water when they are closed and even though their opening area is larger than top-hinged gates they are still mostly closed. Like traditional gates, Side-hinged gates limited mixing (Giannico and Souder 2005)

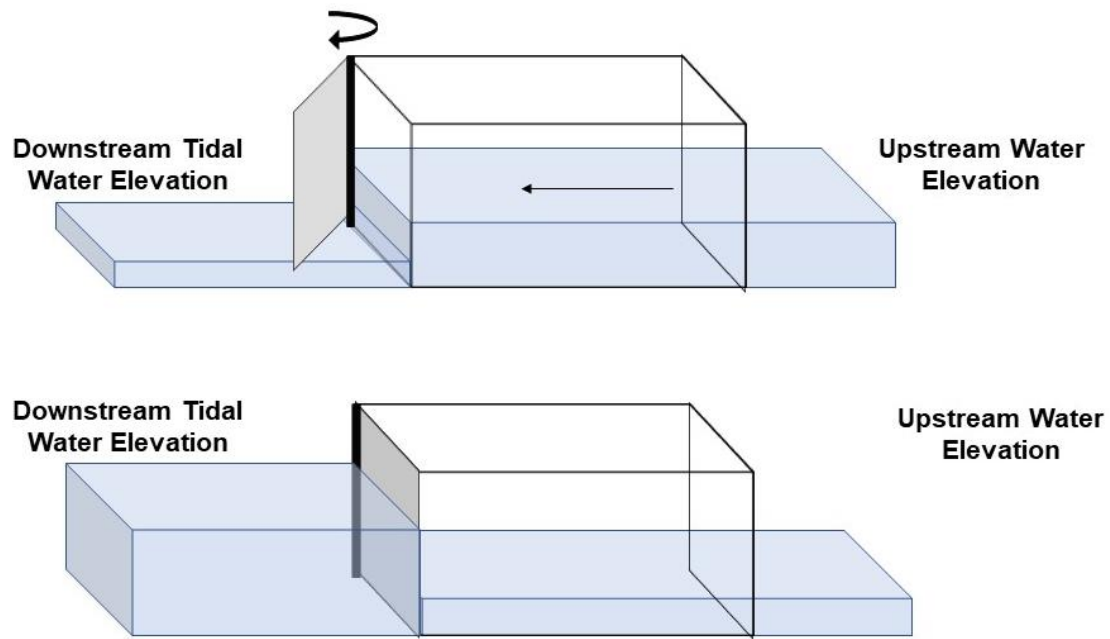


Figure 3. A side-hinged tide gate design demonstrating how the upstream and downstream head differential opens and closes the gate.

Pet Door and Permanent Opening Designs

Pet door and permanent opening modifications place a smaller gate or permanent opening within a larger gate to allow for tidal mixing and fish passage when the primary gate structure is closed. Figure 4 shows the various types of pet doors/permanent openings placed on tide gates. The pet door modification can itself be top-, bottom- or side-hinged. An additional modification is a sliding pet door which allows for a permanent opening to be adjusted by hand to customize leakage. Top-hinged and side-hinged pet doors open due to the upstream and downstream head differential. Because both top- and side-hinged pet-doors are closed by default, they allow for less tidal mixing

compared to the bottom-hinged door or permanent opening. The bottom-hinged pet door only closes when an attached float on the downstream side of the gate rises to a set level that closes the gate. Pet doors and permanent openings can be customized for each site to enhance passage and water quality by design of their size and closing criteria (Giannico and Souder 2005).

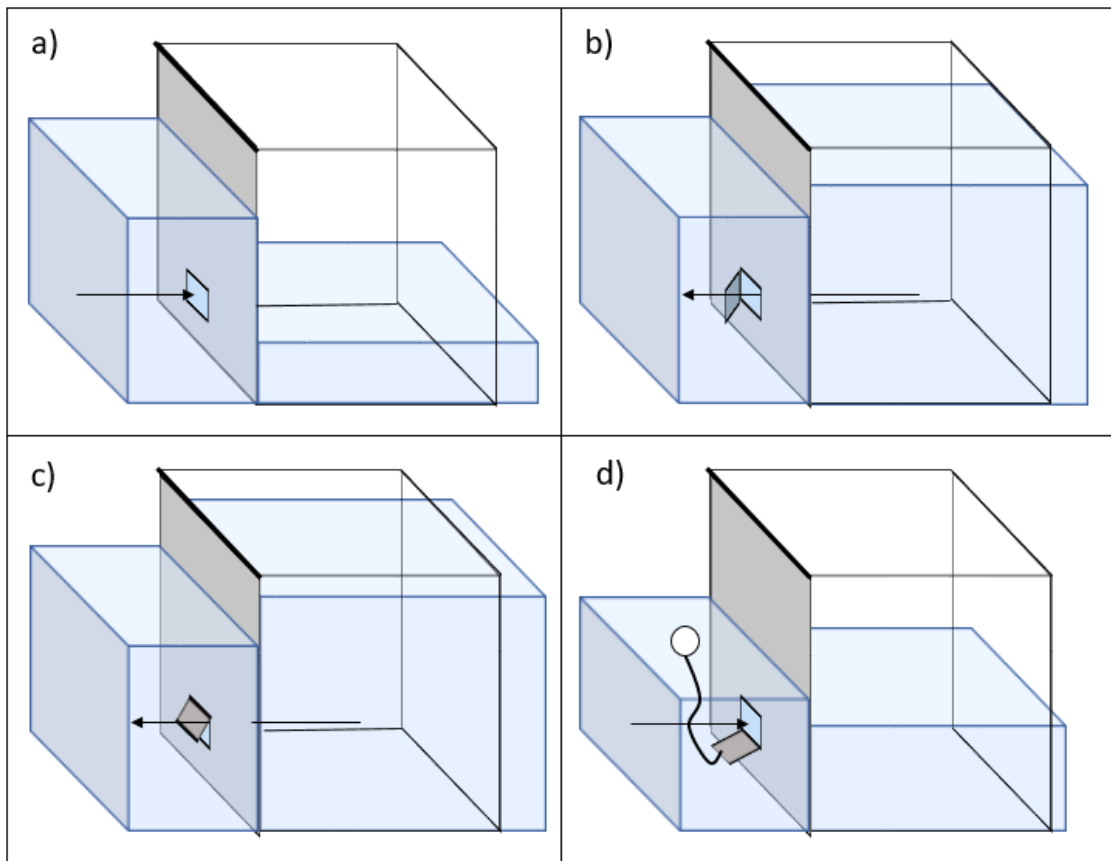


Figure 4. Diagrams of an a) permanent opening, b) aside-hinged pet door, c) a top-hinged tide gate and d) a bottom-hinged tide gate.

Effects of Tide Gates on Ecology and Habitat

The installation of tide gates greatly impacts the ecology and habitat of the surrounding areas. Tide gate structures affect channel geometry, water quality and soils upstream of the tide gate. These can negatively impact species that were present before the tide gate installation and alter the habitat (Giannico and Souder 2005). Various fish species rely on brackish estuarine habitat as a full-time habitat or to transition from fresh water to saline water as juveniles. Threatened species present in Humboldt Bay and relying on healthy estuaries for some or all life stages include steelhead trout, coho and chinook salmon and the tidewater goby (USFWS 2013b). Studies that examine how tide gates have affected passage times and water quality and hydraulic conditions in areas influenced by tide gate are summarized below.

Tonnes (2006) compared water quality characteristics and species presence at three sites in Washington State's Snohomish River Estuary (Smith channel, Deadman Slough, and Otter Island channel). The Smith channel and Deadman Slough had traditional, top hinged tide gates. The Otter Island channel did not have a tide gate and acted as a reference channel. Channel bottom temperature, surface salinity and surface DO were measured between March and September at each site at various tidal heights. Temperature data was separated into two periods covering March through May and June through September. Tonnes (2006) noted that temperature can be affected by tide gates due to shallower depths upstream of the gate and because typical upstream land-use upstream removes vegetation that can provide shade. Otter Island's minimum mean

temperatures for both periods were 1 °C and 0.7 °C lower than Deadman Slough.

Minimum mean temperature differences were 3.1 °C and 1.7 °C lower at Otter Island than at Smith channel. Table 1 shows percent time that the water temperatures were within the growth boundary for juvenile Chinook salmon and when the temperatures were too high that they were stressful and/or lethal. Between June and September, the channels with tide gates were much more likely to have temperatures that are stressful or lethal to juvenile Chinook salmon.

Table 1. Percent time water temperatures were within various growth boundaries for juvenile Chinook salmon. Table adopted from Tonnes (2006).

Channel	Lower Growth Boundary (4.5°C-10°C) % Time	Optimal Growth Boundary (10.0°C-15.6°C) % Time	Upper Growth Boundary (15.6°C-19°C) % Time	Stressful (19°C-23°C) % Time	Potentially Lethal (23°C-26°C) % Time
Otter	1.6	27.0	32.5	38.9	0.1
Smith	0	0.02	36.4	57.9	5.7
Deadman	0	19.7	33.9	43.3	3.5

Salinity and DO were measured using hand-held instruments during high and low tide between March and June of 2003 in the Smith and Otter Island channels and at Union Slough located near the outlet of Smith Channel's tide gate. Seven spot measurements were taken at the Smith and Otter Island channels and five measurements were taken at Union Slough. Salinity increased from 1 to 6 ppt in the Smith Channel over the measurement period. Salinity measurements ranged between 0 and 2 ppt values at the Otter Island channel and Union Slough. The Smith Channel was the only salinity sampling site located upstream of a tide gate. Tonnes (2006) states that increased salinity

could be a result of inorganic dissolved solids, warmer temperatures, fertilizer discharges, stratification and evaporation. DO ranged between 3.8 and 10.2 mg/L at the Smith channel and 7.3 and 10.6 mg/L at the ungated Otter Island channel. Tonnes (2006) stated that the DO measurements were limited, but there was a greater variation of measurements at the Smith Channel.

Tonnes (2006) study also examined species richness in the two gated channels (Smith Island channel and Deadman Slough) and two natural reference channels (Otter Island channel and Deadman Slough downstream of the tide gates). Fyke nets were set across each channel cross section to capture fish exiting each area. The un-gated reference channels had nine species captured, while the gated channels only had three. Additionally, 430 fish in total were captured along the gated channels while 1,599 fish were captured in the tidally influenced channels.

Another Washington and Oregon study found that both traditional, top-hinged gates and “fish-friendly” self-regulating tide gates resulted in decreased connectivity and salinity and temperature that negatively impacted anadromous fish (Greene et al. 2012). Greene et al. (2012) performed a spatially extensive study comparing water quality and passage between “fish-friendly” tide gates, flap gates and natural, reference sites. Five systems throughout Washington and Oregon were studied, with each system having one flap gate, one reference site and between one and three “fish-friendly” tide gate sites. Physical monitoring occurred by deploying water level, salinity and temperature loggers upstream and downstream of each tide gate. Tilt sensors were also connected to the tide gates. Monitoring took place between March and July 2011. Additional velocity

monitoring took place in June and July of 2011. Biological monitoring occurred to sample fish, amphibians and small and large invertebrates. Connectivity was measured over 24-hour periods and measured the amount of time a gate was “passable”. The gates were “passable” when the gates were open and the downstream water level was not more than 10 cm below the downstream culvert invert. The spatially extensive study found that connectivity was reduced by 50% when comparing a “fish-friendly” gate to the reference site and 75% when comparing a flap gate to the reference site. The connectivity results are an average of daily results measured between March and July 2011. Greene et al. (2012) did not provide values for time open but provided plots of the results shown in Figure 5.

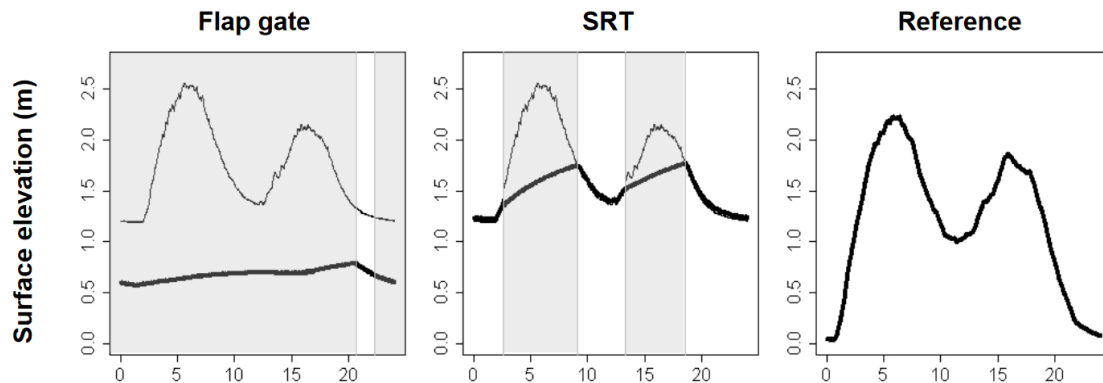


Figure 5. Connectivity results from Greene et al. (2012) showing time (hours) versus surface elevation (meters). Shaded areas represent when gates were closed. Results for the flap gate and the SRT show water surface elevation downstream (thin line) and upstream (bold line) the tide gates. Figure adopted from Greene et al. (2012).

Greene et al. (2012) also performed a temporally intensive study on three sites and compared restoration effectiveness. The sites were monitored pre- and post-

restoration and all sites included installing “fish-friendly” gates. At one site, Chinook salmon densities increased six times after installation of a fish-friendly gate but were still eight times lower when compared to a reference site. Another site showed decline in Chinook densities after restoration. The authors noted that monitoring was limited to one year and additional construction upstream of the site may have resulted in unrepresentative results. Overall, Green et al. (2012) stated that both the spatially and temporally extensive studies showed that an SRT greatly reduced habitat and connectivity compared to the reference site. The SRT site was more similar to the flap gate site than the reference site when comparing various results (temperature, salinity, richness and connectivity).

Gate Design Criteria

Historically, tide gate design methods were developed primarily to protect upstream land from flooding. However, many states have begun to implement regulations to provide fish passage or habitat rehabilitation for sensitive species (CalFish 2018). This has resulted in additional considerations when designing tide gates that provide habitat for sensitive species. Traditional and fish-friendly tide gate design requirements and criteria are summarized below.

General Tide Gate Design

Tide gate design will vary depending on the location and requires site-specific data to properly prevent water from flooding the designated upstream area. Design and sizing

for all tide gates requires site physical and hydraulic data to properly size the gate and determine its set elevation within the channel. The primary data needed for all tide gate designs are:

- a local tidal curve,
- stage-storage curve for the channel upstream of the tide gate,
- a maximum water surface elevation upstream of the tide gate that cannot be exceeded,
- the drainage flow rate of the upstream area.

Storm frequency used to calculate the drainage flow rate will vary depending on the type of land use upstream of the tide gate. In California, agriculture makes up a majority of land use upstream of tide gates. General storm frequencies vary depending on the land use and increase as the value increases. Common storm frequencies used are a two-year frequency for pastures, a five-year frequency for rotated crops and a ten-year frequency for intensive truck crops. The maximum surface elevation plus a factor of safety is used to determine the elevations at which the gate will be opened. Determining the elevation for gate closure requires computing the hourly storage volume and its corresponding stage for the channel upstream of the tide gate. This relationship can be compared to the tidal stage data to determine when the gate closes on a flood tide limb. The gate should close when the tidal stage and hourly storage stage are equivalent (USDA 1971).

Tide Gate Passage Requirements

Federal, state and local agencies recognize the importance of passage requirements for anadromous fish passing through tide gates and are developing design criteria to mitigate the impacts of tide gates. Passage requirements in California are currently based on requirements for hydraulic designs in riverine systems. Aaron Beavers of the National Oceanic and Atmospheric Administration (NOAA) has stated that assuming fish behave similarly in riverine and estuarine settings may lead to tide gate designs that are not optimized for fish passage in the complex and variable hydraulic and water quality conditions that exist within estuaries. Behavior of fish in estuarine settings has not been well studied and may not be similar to behavior of fish in riverine settings (CTC & Associates 2016).

The California Department of Fish and Wildlife (CDFW) and the National Marine Fisheries Service (NMFS) define flow, water velocity and depth criteria for passage of anadromous salmonids, non-anadromous salmonids, native non-salmonids and non-native species (CDFG 2004; NMFS 2001). The high and low design flows (Table 2 and

Table 3) are defined to match peak migration conditions for in-channel flows. Each design flow has a second set of criteria that can be used if data for percent annual exceedance flow is not available. For the low design flow, the alternate minimum flow should be used if it is greater than the percent annual exceedance. The high design flow boundary is used to determine the velocity and depth design criteria (Table 4 and Table 5) are set so that hydraulic conditions in structures do not exceed the swimming capabilities for the target species or age class.

Table 2. High design flow criteria for fish passage in culverts for salmonid and non-salmonid species set by the California Department of Fish and Wildlife. Table adapted from (CDFG 2004).

Species/Life Stage	Percent Annual Exceedance Flow	Percentage of 2-year Recurrence Interval Flow
Adult Anadromous Salmonids	1%	50%
Adult Non-Anadromous Salmonids	5%	30%
Juvenile Salmonids	10%	10%
Native Non-Salmonids	5%	30%
Non-Native Species	10%	10%

Table 3. Low design flow criteria for fish passage in culverts for salmonid and non-salmonid species set by the California Department of Fish and Wildlife. Table adapted from (CDFG 2004).

Species/Life Stage	Percent Annual Exceedance Flow	Alternate Minimum Flow (cfs)
Adult Anadromous Salmonids	50%	3
Adult Non-Anadromous Salmonids	90%	2
Juvenile Salmonids	95%	1
Native Non-Salmonids	90%	1
Non-Native Species	90%	1

Table 4. Maximum velocity and minimum depth criteria for fish passage in culverts for salmonid set by the California Department of Fish and Wildlife. Table adopted from (CDFG 2004).

Species/Life Stage	Maximum Average Water Velocity (fps)	Minimum Flow Depth (ft)
Adult Anadromous Salmonids	See Table 5	1.0
Adult Non-Anadromous Salmonids	See Table 5	0.67
Juvenile Salmonids	1	0.5

Table 5. Maximum velocity criteria for fish passage in culverts for adult salmonid set by the California Department of Fish and Wildlife. Table adopted from (CDFG 2004).

Culvert Length (ft)	Adult Non-Anadromous Salmonids (fps)	Adult Anadromous Salmonids (fps)
<60	4	6
60-100	4	5
100-200	3	4
200-300	2	3
>300	2	2

NMFS's defines adult and juvenile fish passage criteria for salmonids that are similar to the CDFW criteria (NMFS 2001). NMFS' maximum average velocity per culvert length for adult salmonids, low and high design flows, maximum average velocity for juveniles, and minimum depth requirements for adult and juvenile salmonids are the same as the CDFW.

The above standards are currently applied to various components of a tide gate, including the culvert barrel, the gate, and additional openings such as a pet door or a permanent opening. Each component has a different function and applying the same standards to each one could potentially lead to problems within the design. Additionally, the above standards largely emphasize passable flows. A tide gate system can experience a large range of flows within one tidal cycle not all of which are passable; thus, the duration of passable conditions could be limiting.

Fish passage requirements for tide gates are under development and design standards for tide gates that allow for fish passage have not been officially adopted in

California. The Oregon Department of Fish and Wildlife have implemented the following design requirements for tide gates:

- Tide gates must be a minimum of 4 feet wide.
- Tide gates must be open at least 12 inches during passage times.
- Hydraulic drops cannot exceed 6 inches for juveniles or 12 inches for adults.
- Velocity cannot exceed 8 feet per second through the gate and 2 feet per second within the upstream culvert.
- Water depth in the culvert must be 6 inches for juveniles or 12 inches for adults.
- Hydraulic criteria stated above must be met during at least 51 percent of tidal cycles.

These criteria apply for tide gates within streams that require passage of anadromous fish species (Stahl 2006).

NOAA is currently working on passage requirements for tide gates that will be a part of the NMFS's Anadromous Salmonid Passage Facility Design. Draft NMFS passage requirements are listed below (Novak and Goodell, 2006):

- Velocity in culvert is less than 1 foot per second.
- Hydraulic drop cannot exceed 6 inches for juveniles or 12 inches for adults.
- Water depth in culvert must be greater than 1 foot.
- Gate must be open 1.5 feet or more to be considered "open".

- The above criteria must be met at least 90 percent of the time when the gate is open.

Velocity, hydraulic drop and water depth criteria for tide gates are the same as culvert criteria previously summarized.

Tide Gate Hydraulic Analysis

Tide gate hydraulics are not well studied and limit modeling capabilities and introduce uncertainties in design and analysis. The following section describes tide gate hydraulic characteristics, modeling methods, and parameters that have been used for design and analysis of tide gates.

Total Head Loss

Culverts are a hydraulic system with supporting research that are comparable to tide gate installations and culvert loss coefficients are often used to simulate tide gate energy losses. The energy equation can be used to determine the total head loss (H_L) when the upstream and downstream velocity, depth and elevation are known (Schall et al. 2012).

$$HW + LS + \frac{V_u^2}{2g} = TW + \frac{V_d^2}{2g} + H_L \quad (\text{Eq. 1})$$

Where:

HW = headwater depth (ft)
 LS = elevation difference through culvert (ft)

$$\begin{aligned}
 V_u &= \text{upstream velocity (ft/s)} \\
 V_d &= \text{downstream velocity (ft/s)} \\
 H_L &= \text{total energy (head) loss (ft)}
 \end{aligned}$$

The total energy loss incorporates losses due to friction, entrance and exit losses, or geometry changes (bends for example). The individual losses can each be calculated based on hydraulic characteristics through the system and coefficients based on the geometry type (Schall et al. 2012).

The total energy loss for a tide gate system can be estimated using the same approach as the total energy loss for a culvert. The tide gate system, however, will have an additional loss due to the gate. Figure 6 shows entrance, friction and exit losses through a culvert/tide gate system. The tide gate loss can be estimated once the total energy loss is determined, and the other losses are estimated and subtracted from the total.

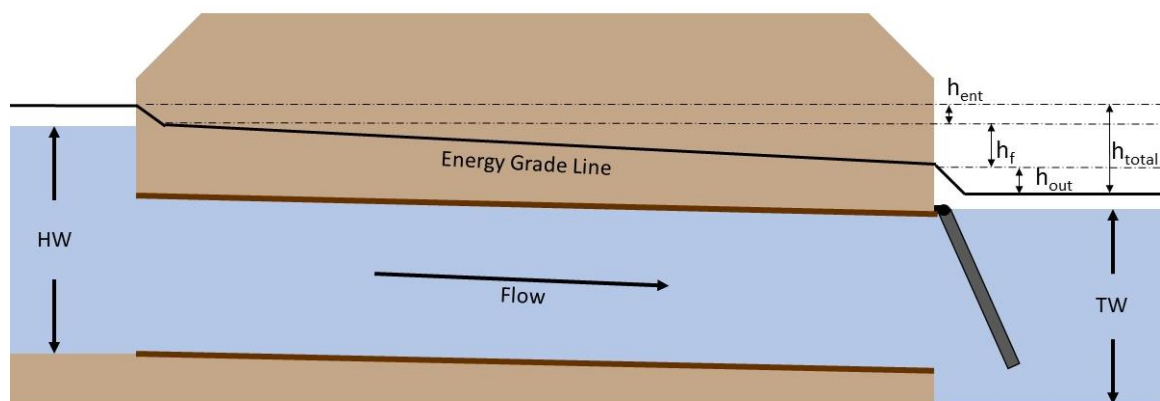


Figure 6. Energy grade line showing the decline through the culvert and gate. Figure shows losses due to the culvert entrance, friction losses and outlet losses. Outlet losses comprise of culvert outlet and tide gate losses.

Energy Loss Coefficients

In an open-channel tide gate system, total head loss can be calculated by looking at the change in elevation head between an upstream and downstream point. Energy loss is defined as a pressure decrease within a system due to channel characteristics and barriers within a channel and how they impact flow. Multiple components within a tide gate system can attribute to head loss. Common components include culvert entrances, channel friction, and tide gates. Energy loss coefficients can be used to estimate how specific components within a system are attributing to head loss. Energy loss coefficients are dimensionless numbers that have been experimentally calculated to determine how common components will impact head loss. These coefficients can then be applied to similar systems and estimate head loss depending on velocity through the channel of interest. Tide gate energy loss coefficients have not been studied enough to be readily applied to multiple gates. The lack of direct measurement of tide gate energy loss coefficients results in uncertainty in the hydraulic modeling of tide gate systems (CTC & Associates 2016). Previous studies of hydraulic models of tide gates rarely determined the energy loss coefficients and use values for similar structures (i.e., culverts) when coefficients were needed for developing models for design and analysis.

Head Loss and Loss Coefficients for Gates and Similar Structures

Replogle and Wahlin (2003) studied how flap gate (top-hinged gate) head loss in drain pipes change with the opening angle and weight of the gate. Replogle and Wahlin

initially derived a head loss versus flow equation of “light” flap gates with pin-type hinges based on data compiled by the Soil Conservation Service (SCS):

$$\frac{H_L}{D} = \frac{1}{176} \frac{gD^5}{Q^2} \quad (\text{Eq. 2})$$

Where g is the gravitation acceleration constant, H_L is head loss (m or ft), D is pipe diameter (m or ft), and Q is discharge rate (m^3/s or ft^3/s).

Their experiment used a 20-cm diameter pipe with an elastic-hinged flap gate angled approximately 15 degrees from the vertical and an elliptical outlet to determine if it would produce similar results to Equation 2. Piezometers were placed at 30.5 cm intervals to measure pressure change over the length of the pipe. Various flows were discharged through the gated pipe without any weights on the gate, with one 2 kg weight on the gate, and with two 2 kg weights on the gate. Figure 7 shows head loss versus flow results for the pin-type hinge gate using Equation 2 and those measured for the three elastic hinge gate variations.

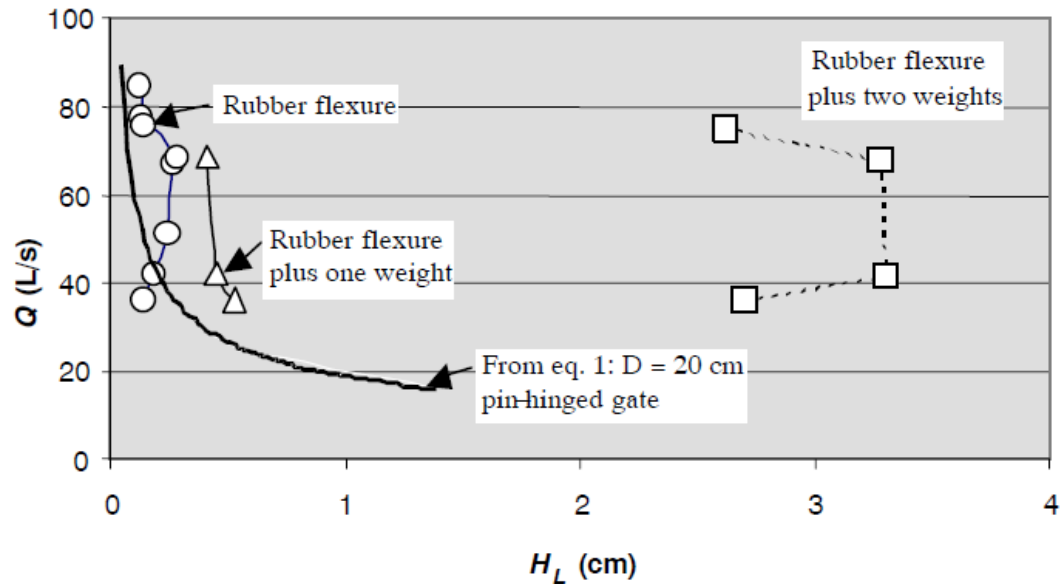


Figure 7. Head loss versus flow results for the SCS calculated head loss for pin-hinged gates and laboratory tested rubber flexure (elastic) hinges. Adopted from Replogle and Wahlin (2003).

From Equation 2, the head loss decreased as the discharge increased and approached zero at higher flow rates. For the rubber hinges, head loss remained fairly constant regardless of flow rate. The gate with two weights experienced the greatest head loss and had more variety in head loss values compared to the lighter gates (Replogle and Wahlin 2003). Results from this study showed that as the weight of the gates increased, so did the head loss. Additionally, from the pin-hinged gates, lower flow rates resulted in higher head loss most likely due to having to overcome the hydrostatic force at lower flows.

Replogle and Wahlin (2003) also examined head loss behavior of the gates compared to the opening angle of the gate. The angle was measured from the vertical

axis. Figure 8 compares head loss with respect to the velocity head versus gate angle opening for the elastic-hinged gates with various weights for a free outfall. The graph also showed results from a previous study performed by Burrow and Emmonds (1988). The Burrow and Emmonds (1988) results were under submerged conditions where the elevation of the water and pipe top were equal. Additionally, Figure 8 shows Burrow and Emmonds' results as an average between various sized gates. Replogle and Wahlin's results showed minimal changes in head loss over the various opening angles for the gate without added weight and for the gate with one added weight. Head loss for the gate with two added weights was larger at smaller angles and decreased as the angle increased. Replogle and Wahlin stated that this was most likely due to the heavier gate requiring a larger velocity head to overcome the hydrostatic pressure. Burrows and Emmonds' results had a larger head loss and a greater gate opening angle range. Replogle and Wahlin (2003) stated that the greater head loss values are most likely due to submerged conditions. The range in gate opening angles is most likely due to buoyant forces on the gate under submerged conditions.

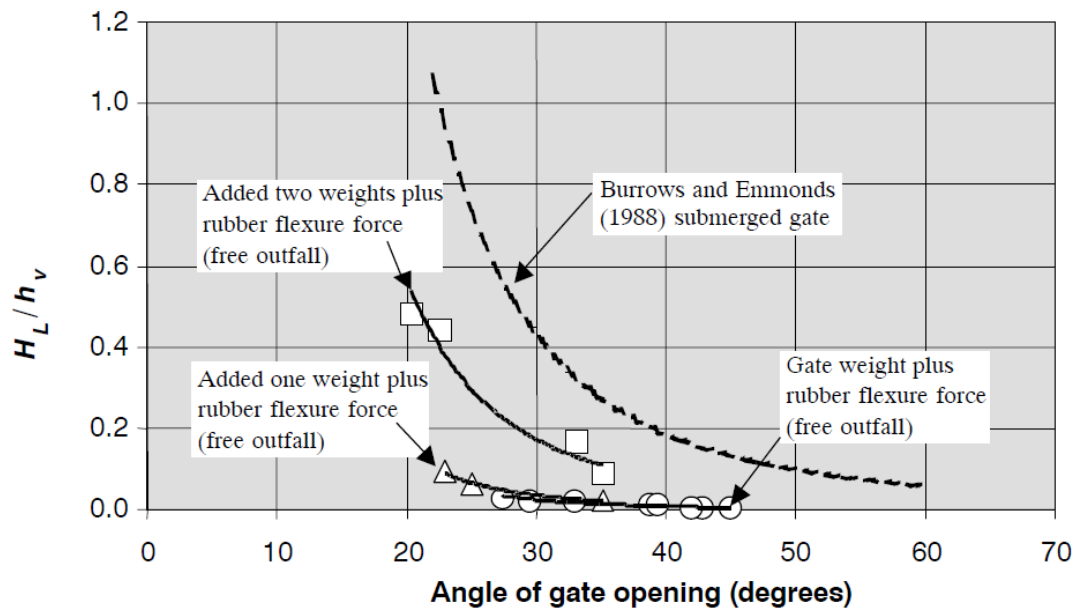


Figure 8. Head loss relative to velocity head versus angle of gate opening for laboratory tested rubber flexure (elastic) hinges with various gate weights. Adopted from Replogle and Wahlin (2003).

Simulating Tide Gates in Hydrodynamic Models

Many hydrodynamic models include components that are used to approximate tide gate hydraulics. Three hydraulic models and studies illustrating their application in tidally influenced systems and assumptions needed to model tide gates are described here and the methods and coefficients used to simulate tide gate hydraulics are highlighted.

HEC RAS 1D

The US Army Corps of Engineers' one-dimensional Hydrologic Engineering Center River Analysis System (HEC-RAS) software is commonly used to model tide gates. HEC-RAS has the ability to model tide gate systems using lateral or inline structures. Radial gates (flap gates) or sluice gates can be placed within these structures

and are modeled using a combination of weir and gate flow depending on upstream and downstream conditions (Brunner 2012). The software does not allow for input of variables, such as energy loss coefficients and gate closure rates (CTC & Associates 2016).

Novak and Goodell (2006) modeled the Kentucky Slough tide gate system in Coos Bay, Oregon using HEC-RAS to determine when the draft NMFS hydraulic passage requirements were met. A one-dimensional, unsteady flow model was developed in HEC-RAS 3.1.3 using a sluice gate to represent a side-hinged tide gate. The model was run using multiple scenarios to simulate a large range of conditions. Altered variables included dimensions of the culvert and tide gate, and the upstream channel characteristics. An upland inflow of 1.0 cfs and a two-day tidal cycle for Coos Bay measured in August 2006 was used as the downstream boundary.

Novak and Goodell (2006) noted that the difficulties with HEC-RAS mainly focused on the lack of inputs that are needed to accurately model a tide gate. Limitations included:

- Manually creating a gate opening schedule.
- No options for gate types other than flap or sluice.
- Only one discharge coefficient could be applied throughout the various gate opening.

The desired gate controls were to have the gate open until the upstream water elevation reached a design tide inundation elevation (DTIE). The DTIE occurred when

the downstream water elevation was above the upstream water elevation, creating a negative head. To recreate this gate schedule, Novak and Goodell initially ran the model where the gate was open until the downstream water level was above the upstream water level. The results were exported and the gate opening schedule was manually altered over two to three trials. When the model was running, only one discharge coefficient could be used. Novak and Goodell (2006) stated that because a sluice gate was used to model a tide gate and they have different mechanical operations, the model lost accuracy.

HEC-RAS was also used for the Martin Slough Enhancement Project in Humboldt County, California. Prior to the enhancement project, the Martin Slough habitat had been severely impacted by land-use changes and traditional tide gates installed between Martin Slough and Swain Slough. The purpose of the enhancement project was to improve fish passage by replacing the traditional tide gates with three new gates plus an auxiliary door, increase the amount of riparian corridor, reduce flood impacts, improve sediment transport, improve water quality, and increase diversity and freshwater habitat. Love et al. (2013) created a HEC-RAS model to run various simulations to determine the dimensions and settings of the tide gates, assessing fish passage, determining flooding conditions, assessing sediment transport, and evaluating salinity. This was a large project and the tide gate replacement was just one aspect of it. The following summary focuses only on how the HEC-RAS model was used to model the tide gates.

The new tide gate system at Martin Slough contained three 6-foot by 6-foot tide gates with a smaller 2-foot by 1.5-foot auxiliary door included in the middle gate. The

outer, larger tide gates are side hinged, and the middle tide gate and the auxiliary door are top-hinged. The southern side-hinged gate and the auxiliary door have a muted tide regulator (MRT). The MRT uses a lever and a float to allow a gate to remain open longer, even when the downstream water level is higher than the upstream water level. The tide gates and the auxiliary door were modeled in HEC-RAS as lateral structures. For outgoing flows, the tide gates were treated as three concrete culverts with flap gates that would prevent the downstream tidal water from entering upstream. For incoming flows, the MRT gate and auxiliary door were treated as sluice gates. The sluice gates were given a discharge coefficient of 0.6 and closed when the downstream elevation was 4 feet for the gate and 5.7 feet for the auxiliary door (Love et al. 2013).

Various model scenarios were run and each had a purpose related to a particular design aspect of the entire Martin Slough Enhancement Project. Scenario 7 was a 331-day simulation that modeled variation throughout the year. The freshwater inflow was measured annual inflow hydrographs and the downstream boundary was based on the annual tide records. Scenario 7 was used to verify that the tide gate dimensions and MRT settings allowed for a muted tide, while still preventing upstream flooding. Scenarios 8 through 11 model fish passage conditions over a 365-day simulation. Low and high fish passage design flows for juvenile and adult salmon and steelhead were set as the freshwater inflow and the downstream boundary was based on the annual tide elevations. Table 6 and Table 7 shows the percent time passable for each design flow when the gates are open (Love et al. 2013).

Table 6. Percent time passable for upstream and downstream movement based on juvenile salmon and steelhead design low and high flows. Table adopted from Love et al. (2013).

Design Flow	Stream Flow	Percent of Time Gates Open	Percent of Time Passable Upstream	Percent of Time Passable Downstream
Low Passage Design Flow	1 cfs	98.3%	98.1%	54.7%
High Passage Design Flow	27 cfs	95.5%	94.3%	64.7%

Table 7. Percent time passable for upstream and downstream movement based on adult salmon and steelhead design low and high flows. Table adopted from Love et al. (2013).

Design Flow	Stream Flow	Percent of Time Gates Open	Percent of Time Passable Upstream	Percent of Time Passable Downstream
Low Passage Design Flow	3.6 cfs	95.5%	92.8%	78.9%
High Passage Design Flow	89 cfs	91.7%	91.7%	91.7%

SWMM

The Environmental Protection Agency's Storm Water Management Model (SWMM) is an open-source model mainly used to model urban runoff systems. SWMM is capable of performing hydrologic, hydraulic and water quality simulations for single or continuous events. Capabilities related to hydraulic tide gate modeling include flow routing. SWMM uses Saint Venant flow equations to allow for steady flow, kinematic wave and dynamic wave routing (Rossman 2015).

A SWMM model was modified by the United State Geological Survey (USGS), in cooperation with U.S. Fish and Wildlife, to determine how hydraulic structures would impact flood management in Virginia Beach, VA (Keaton 2004). Lake Tecumseh and its

surrounding wetlands have been impacted by development and canal-dredging which has resulted in tidal waters regularly entering the lake and wetlands. Major consequences of this include a decrease in Lake Tecumseh stormwater storage capacity, transformation of wetland types, and increases in turbidity that result in less aquatic vegetation (Keaton 2004).

The updated model was used to determine if installing flap (top-hinged) gates along the main canal, Canal 1, or installing weirs along the outlet of Lake Tecumseh would better restore Lake Tecumseh and its surrounding wetlands. The tide gate scenario included installing 20 parallel unidirectional flap gates on the end of 20 box culverts that were each 4-ft by 2-ft and had an invert elevation of 2.2 ft. SWMM does not allow for more than 15 junctions to be modeled for a single node, so the flap gates were divided between two flow paths. It was assumed that once the water level elevation rose above 2.2 ft, the gates would close, and the closed gates would act like a 200-ft wide weir at an elevation of 6.2 feet (Keaton 2004). Head loss was accounted for in the model when the gates were open by assigning an overall head loss coefficient (K_L). It was assumed that K_L was 1.0. The weir scenario set transverse horizontal weirs along the outlets of Lake Tecumseh to Canal 1. The invert elevation of the weirs was at 2.2 ft.

The SWMM model was run for each hydraulic structure scenario and peak water-surface elevations at each node were compared to the baseline conditions. For the tide gate scenario with the median initial water surface elevation, the average difference over all the design storms was +/- 0.1 ft with some outliers. Outliers only occurred in design storms greater than 10 years. The largest outlier (1.3 ft) occurred during the 25-year

storm and the node showed numerical instability. However, instability only occurred at certain locations for small amounts of time and the authors did not believe it affected the overall results (Keaton 2004).

Telemac2D

Another program that has been used to model tide gate hydraulics is Telemac2D. Telemac 2D is an open-source software initially created by the Laboratoire National d'Hydraulique et Environnement (LHNE) of the Research and Development Directorate of French Electricity Board (EDF-R&D) and is currently maintained by various consultants and research institutes. Telemac2D solves Saint Venant equations to model two-dimensional maritime and riverine systems (Lang et al. 2014).

Cassan, Guiot and Belaud (2018) used Telemac 2D to evaluate discharge coefficients using numeric and experimental lab methods for a theoretical side-hinged gate. Discharge coefficients estimated using the numeric methods were verified through the experimental methods. The purpose of this study was to develop an accurate hydraulic model to aide in implementing stiffeners or blockers for fish passage that would allow for longer passage times. The study did not have a specific area of interest, but wanted to evaluate how side-hinged gates commonly found in French coastal marshes could better facilitate Eel migration while still protecting upstream resources. Stiffeners or blockers are installed on gates to create a resistant force against the gate closing from tidal flows moving upstream. Stiffeners slow the gate closing time, which blocks prevent full closure of the gate. Cassan et al. (2018) began by deriving a theoretical relationship

of the discharge coefficient versus gate opening based on the energy equation (Equation

3). Their analysis assumed no head loss due to velocity head or friction.

$$C_d = C_c \sqrt{\frac{1 - X}{\frac{\alpha_d}{X^2} - (aC_c)^2}} \quad (\text{Eq. 3})$$

Where:

C_d	=	discharge coefficient
C_c	=	contraction coefficient
X	=	water depth ratio between freshwater to tidal water depths
a	=	relative opening
α_d	=	downstream Coriolis coefficient

The discharge coefficient was calculated for two side-hinged tide gates using the altered energy equation, an experimental device and a 2-D shallow water model created using the open-source software, Telemac2D. The first gate (Type A) was a gate that spanned the whole channel width, and the second gate (Type B) spanned half the channel width. The Telemac2D model output the Coriolis coefficient and contraction coefficients for various flows, upstream and downstream water depths and gate angle opening. The Coriolis coefficient varied between 1 and 1.15 over the range of conditions simulated; thus, a Coriolis coefficient value of 1.08 was assumed for use in Equation 3. The contraction coefficient varied between 0.7 and 1.1 for Type A and 0.6 and 0.9 for Type B. For Equation 3, a contraction coefficient of 1 was used for Type A and 0.75 for Type

B (Cassan et al 2018). Figure 9 shows the discharge coefficients for each gate type calculated using the experimental system and the shallow water models.

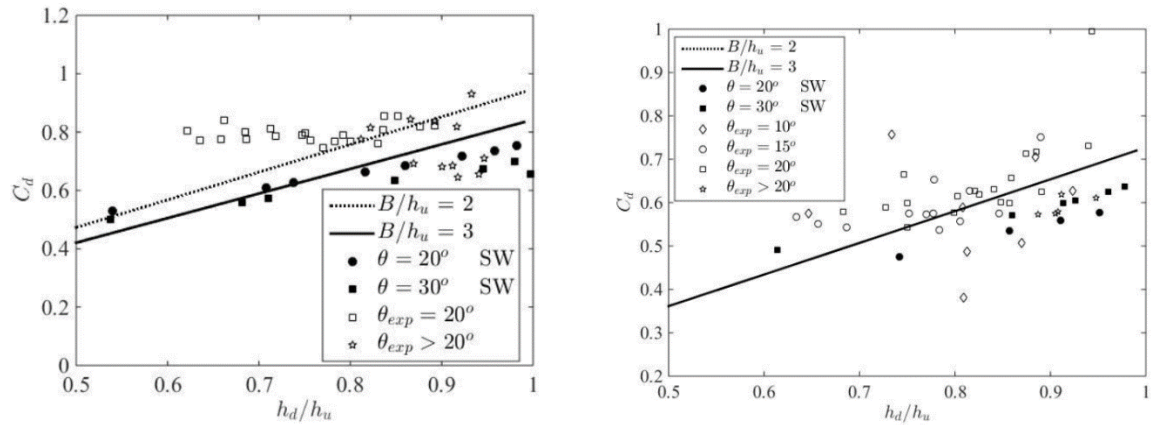


Figure 9. Discharge coefficient versus downstream (h_d) over upstream (h_u) water depth ratio for the shallow water (SW) model and experimental results. Type A results are on the left and Type B results are on the right. B/h_u refers to ratio of the cross-sectional width to the channel depth. Theta refers to the angle of the gate opening. Figure adopted from Cassan et al. (2018).

Cassan et al. (2018) used the calculated discharge coefficients to model the tide gate operation with and without a stiffener under tidal conditions. These results were compared to determine how the stiffener would impact gate opening times. The tidal input was an average modeled tide at the mouth of the Charentes River, France that included the ebb and flood phase over a twelve-hour period. The stiffener was evaluated at three different total device stiffnesses, which is a function of the stiffness of the stiffener and the geometrical configuration of the stiffener. Quasi-steady and unsteady models regarding the presence of hydrostatic pressure were run. Dimensionless flowrate results and angle openings were each compared to time. It was shown that quasi-steady

conditions were similar to the unsteady models and that the quasi-steady results were accurate enough to use (Cassan et al. 2018).

Cassan and his colleagues continued their work on tide gates studying tide gates that use stiffener and float modifications to slow gate closing rates and extend fish passage times (Guiot et al. 2020). The main objective of this study was to model each tide gate type and determine which one resulted in the longest passage time and best limited saltwater intrusion. Their study compared how stiffeners and float modifications worked on a flap gate (top-hinged), a tidal gate (side-hinged), and a self-regulating tide (SRT) gate. The SRT gate utilized in this study has a float that is connected to the gate. The gate is open until the water level increases enough to submerge the float and causes the gate to close.

Modeling of the tide gates included determining the forces and opening geometry for all three tide gate types. To verify that a quasi-stationary solution was sufficient, Guiot et al. (2020) compared the results for the unsteady Equation 4 and the quasi-stationary Equation 5. Equations 4 and 5 describe the volume of tidal water entering the upstream system as the gates are closing. For the quasi-stationary equation (Equation 5) it is assumed that the moment of inertia (J_A) is zero. Results from Equations 4 and 5 were used in Equations 6 and 7 to calculate the dimensionless flow rate.

$$\frac{(1 - X^2)}{4} + \tilde{k}\tilde{l}^2(\tan \theta - \tan \theta^*)(1 + \tan^2 \theta) = -\frac{J_A \ddot{\theta}}{\rho g h_u^2 l^2} \quad (\text{Eq. 4})$$

$$A_1 - A_2 + \frac{1}{2} \tilde{m} \sin \theta \tilde{l} + \tilde{k} \left(\frac{l}{h_u} \right)^2 (\tan \theta - \tan \theta^*)(1 + \tan^2 \theta) = 0 \quad (\text{Eq. 5})$$

$$Q = C_d w h_u \sqrt{2g(h_u - h_d)} \quad (\text{Eq. 6})$$

$$C_d = \frac{F_0}{a} \frac{1}{\sqrt{2(1 - X)}} \quad (\text{Eq. 7})$$

Where:

X	=	ratio of sea level depth over upstream depth
\tilde{k}	=	stiffener constant
\tilde{l}	=	ratio of length from axis to stiffener over sea level depth
θ	=	gate angle opening
θ^*	=	angle at which stiffener is closed
J_A	=	moment of inertia with respect to the axis
A_1	=	F_0 , numerator of Equation 7
A_2	=	$a\sqrt{2(1 - X)}$, denominator of Equation 7
h_u	=	sea level depth, analysis conducted for incoming tide
h_d	=	upstream depth, analysis conducted for incoming tide
C_d	=	discharge coefficient
w	=	opening length
B	=	channel width
F_0	=	$Q^2 / g B^2 h_u^3$
a	=	$\frac{w}{B}$

Figure 10 shows the results comparing the complete and quasi-stationary solutions for different stiffener constants. The solutions are similar and the complete solutions showed numerical oscillations; thus, quasi-stationary solution was determined to be sufficient by Guiot et al. (2020).

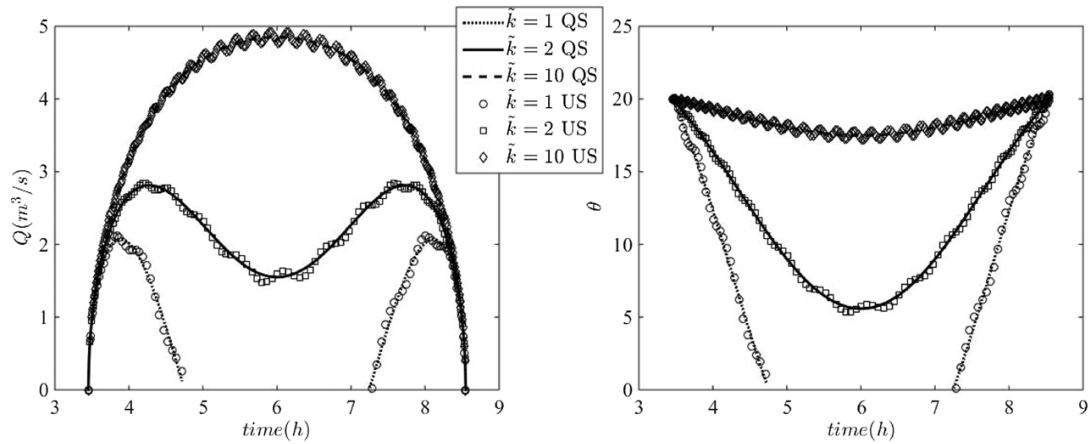


Figure 10. Complete and quasi-steady solutions for flow and gate opening for different stiffener constants. Figure shows two plots with the first (left) showing time versus flow and the second (right) showing time versus theta. Figure adopted from Guiot et al. (2020).

After verification of the quasi-steady solutions, Guiot et al. (2020) modeled each tide gate type with various openings, stiffener constants and placement of stiffeners. The block modification was modeled as a stiffener assuming an infinite stiffener constant and varying the lake of the stiffener to account for size variation. The authors determined passable times by looking at the size of the opening, position of the opening and duration of the opening. Due to the block's design, there was a constant opening in the gate. When comparing a SRT (float system) to tidal and flap gates with a stiffener, the gates with stiffeners had longer opening periods by slowing the gate closing rate. The SRT,

however, maintained larger openings at the beginning and end of the cycle. A larger opening creates lower velocities and more favorable passage conditions.

Guiot et al. (2020) results showed that side-hinged gate allowed for better ecological continuity when compared to flap gates since side-hinged gates maintain a greater range of depth for fish to pass through. Blocks and stiffeners both had advantages and disadvantages. Blocks, unlike stiffeners, were not able to set a maximum volume ratio over various tidal ranges. However, blocks were able to have a constant opening even during high tides and may be favorable to certain species. When comparing floats versus stiffeners, the stiffeners allowed for longer opening times. However, the floats had larger openings and are preferred since they allow larger fish to pass while maintaining lower exchange volume ratios (Guiot et al. 2020).

MATERIALS AND METHODS

The following section describes methods used to perform a hydraulic assessment of two, different tide gate designs. Included is a description of the study sites, data collection methods and analysis methods. Measurements collected for this project were done in conjunction with a tide gate replacement project conducted by the California Department of Transportation (Caltrans).

Study Sites

Gannon Slough and US 101 Slough are two waterways adjacent to the Humboldt Bay that use tide gate structures to prevent upstream flooding. Both gates are owned and maintained by Caltrans. Gannon Slough and US 101 Slough are labeled as critical habitat for endangered or threatened species.

Gannon Slough is located within the City of Arcata limits and is mainly fed by Campbell Creek and Beith Creek. Gannon Slough runs along the eastern side of Highway US 101 and discharges into Humboldt Bay. Three traditional, top-hinged gates were present at the outlet of three box culverts (Figure 11). Each gate was six feet wide by five feet high and the culverts were each 29 feet long. The culvert bottom elevation varied throughout the span of the culvert, but an elevation of 2.33 feet NAVD88 was used in calculations. These gates were replaced with fish-friendly gates in September 2020. The new gates included a new top-hinged gate in the center, two side-hinged gates along on the east and west gates, and a muted tide regulator (MRT) on the eastern gate. Data for

this analysis was collected before the gates were replaced and represent conditions commonly found in traditional tide gates.



Figure 11. Image of the Gannon Slough gates and the downstream (tidal) channel.

US 101 Slough is located in northern Eureka and empties into Freshwater Slough. US 101 Slough runs along Airport Road and the eastern side of Highway US 101. Two aluminum, side-hinged gates are attached to two 82-foot long culverts installed at the mouth of the US 101 Slough. Each tide gate is five feet wide by five feet high (Figure 12). These gates were installed in March 2019 as part of an emergency replacement

project after the old, top-hinged gates failed. Both gates have auxiliary doors that allow for limited tidal inflow to maintain upstream habitat but only the auxiliary door on Gate 2 is currently open.



Figure 12. Image of one of the US 101 Slough gates while it is open. Image taken downstream of the gate. Photo taken by Antonio Llanos.

Data Collection

Daily Monitoring

Continuous monitoring of both sites occurred between May 2019 and June 2020. Each site had four stations that collected water level, surface and bottom temperature, and surface and bottom salinity. Onset Hoboware data loggers were used to collect data at 15-minute intervals. Table 8 provides logger type and model number for each logger. Loggers at each station were housed in a 4-in PVC pipe connected to t-posts placed within the channel (Figure 13). A float was attached to the surface salinity logger to capture the difference in salinity between the surface and bottom of the water. Station One was located downstream of the tide gate, Station Two was just upstream of the tide gate, and Stations Three and Four were further upstream in the slough to capture the extent of fresh and saltwater mixing (Figure 14 and Figure 15). Station Three and Four of Gannon Slough and Station Four of US 101 Slough also included dissolved oxygen sensors and measured surface dissolved oxygen. The water level loggers are pressure transducers that require atmospheric pressure data to convert to a water depth. An atmospheric data logger was on the banks near Station 2 of US 101 Slough. This data was used to process both Gannon and US 101 data water surface elevation.



Figure 13. Image of a field crew member downloading loggers next to the stand-pipes holding water level, salinity and DO loggers at Gannon Slough Station 4.

Prior to the loggers being deployed, t-posts were installed at each station to hold the standpipes. The top of each t-post was surveyed in the NAVD88 vertical datum using benchmarks provided by Caltrans. The reference elevations were then used to determine the water surface elevation. The loggers were downloaded monthly. The reference water level was measured at each station during the 15-minute mark. Each logger was downloaded and placed back within the station. Data collection also included surface and bottom spot measurement of DO, salinity, temperature and pH using a handheld YSI

meter. After all the stations at both sites had been downloaded, the atmospheric logger was downloaded to capture the whole time period.

Table 8. Data loggers used to monitor water level, conductivity and dissolved oxygen. Data Loggers were manufactured by Onset.

Logger	Model Number	Description
Water Level (13 ft) – U20L Series	U20L-04	Water Level
Conductivity Logger 100-55,000 μ S/cm	U24-002-C	Conductivity, Temperature
Dissolved Oxygen Data Logger	U26-001	Dissolved Oxygen

Tilt sensors were custom made for this project to measure the angle of the gate opening at 15-minute intervals. The tilt sensors were comprised of an accelerometer to measure the top-hinged gate opening angle and a magnetometer to measure the horizontal opening of the side-hinged gates (HSU et al. 2020). The tilt sensors were placed on each gate between April 26, 2020 through May 31, 2020.



Figure 14. Gannon Slough monitoring stations used for daily monitoring between May 2019 and June 2020. All stations measured water level, salinity, and temperature. Stations 3 and 4 also included dissolved oxygen loggers.

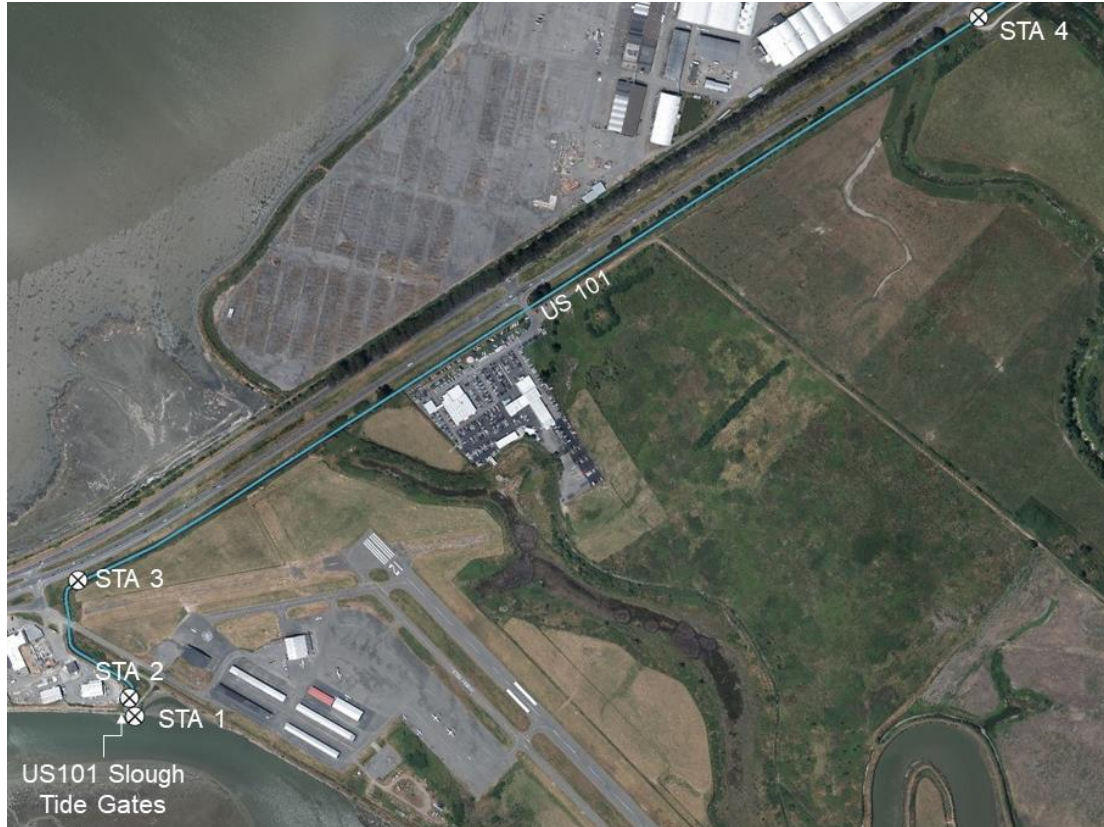


Figure 15. US 101 Slough monitoring stations used for daily monitoring between May 2019 and June 2020. All stations measured water level, salinity, and temperature. Station 4 also included a dissolved oxygen logger.

Velocity and Discharge Measurements

Discharge and velocity measurements were performed at Gannon Slough on October 25, 2019, December 8, 2019, and May 18, 2020. US 101 Slough discharge and velocity measurements were performed on November 10, 2019 and June 10, 2020. The purpose of these measurements was to collect fine-scaled velocity data and identify flow patterns while the gates are open. Measurements took place during ebb tides to capture

the opening and closing of the tide gates and included collecting discharge, water levels, salinity levels and gate opening angles.

Discharge Measurements

Discharge and velocity measurements were collected using a TRDI RiverPro 1200kHz ADCP mounted onto a rigid trimaran attached to a Real Time Kinematic (RTK) antenna. The ADCP uses acoustic pulses to determine depth and velocity as it moves across the cross section. The ADCP was pulled across the channel at a cross section upstream of the tide gates throughout the ebb tide event to quantify the changes in discharge (Figure 16). ADCP measurements were taken every three to five minutes and the values were linearly interpolated to get discharge and velocity data at 1-minute intervals. A unique discharge value was calculated for each traverse across the channel. The ADCP measurements were taken once the tide gates were open until they were closed, or flow was approximately zero. ADCP measurements for Gannon Slough were taken directly upstream of the box culvert. US 101 Slough measurements were collected approximately 525 feet upstream of the gates due to eelgrass interfering with the ADCP measurements at channel locations closer to the gate inlet.



Figure 16. Image showing how the discharge measurements were taken using the ADCP at Gannon Slough along the upstream cross-section. Additional image showing the ADCP on the rigid trimaran.

Water Level and Gate Angle Measurements

Water level, surface salinity and bottom salinity were also measured during the discharge measurements at one-minute intervals. During the 2019 measurement events,

the one-minute loggers were placed downstream and upstream of the culverts at the existing Stations 1 and 2 (Figure 17 and Figure 18).

For the 2020 measurement events additional water level loggers were used to better define the water level and salinity conditions during ADCP measurements. An additional water level logger set at one-minute intervals was placed within one of the culverts at both sites (See Figure 17 and Figure 18). This was to explicitly measure and isolate the culvert entrance loss from the tide gate effects. For Gannon Slough, a temporary station (Station 1.75) was placed downstream of Station Two but upstream of the culvert. The upstream one-minute loggers were placed in Station 1.75. For US 101 Slough, a temporary station (Station 1.25) was placed downstream of the gate but still within the culvert channel. The downstream one-minute loggers were placed in Station 1.25. Gate opening angles were measured by hand and by the tilt sensors on each gate at 15-minute intervals. Figure 19 compares the daily monitoring setup at both locations to each site's ADCP measurements. Green indicates data that were used in the head loss analysis discussed below.

Gate opening angles were taken throughout the opening as the angle changed. Gate opening angles were measured using a digital angle gauge on the Gannon Slough gates and a homemade compass for the US 101 Slough gates.



Figure 17. Gannon Slough monitoring stations used during angle and ADCP measurements performed on May 18, 2020. Stations 1 and 2 are the permanent data collection stations. Stations 1.25 and 1.75 are temporary stations installed during ADCP measurements.



Figure 18. US 101 Slough monitoring stations used during angle and ADCP measurements performed on June 10, 2020. Stations 1 and 2 are the permanent data collection stations. Stations 1.25 and 1.75 are temporary stations installed during ADCP measurements.

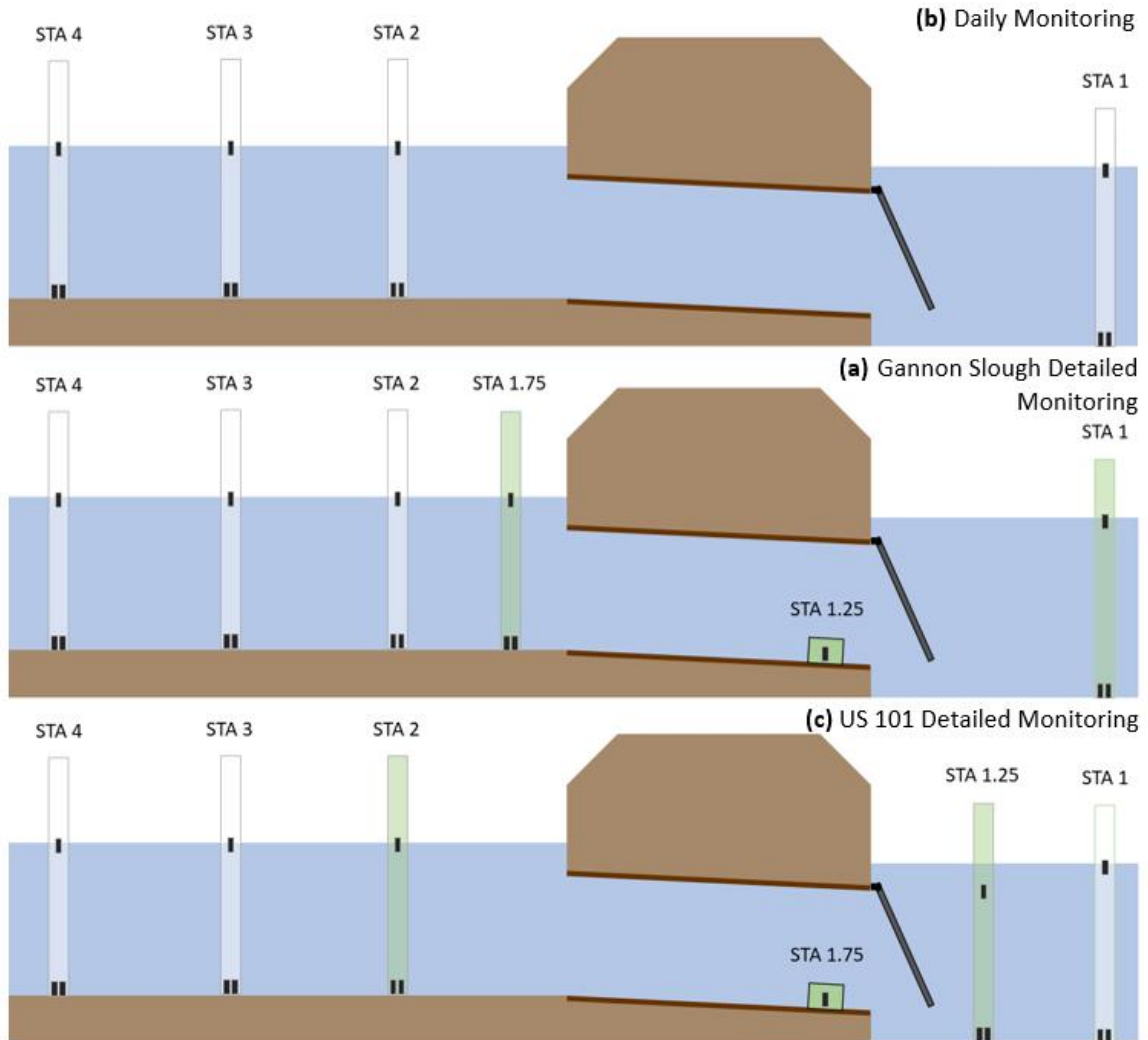


Figure 19. Diagrams comparing the normal monitoring setup compared additional measurements collected during the 2020 ADCP measurement setups at Gannon and US 101 Slough. (a) shows the general monitoring setup used at both locations. Each station has a water level logger, a bottom salinity logger and a surface salinity logger. (b) shows the Gannon Slough setup used on May 18, 2020. The green stations had 1-minute interval loggers and were used for the head loss analysis. The station within the culvert (STA 1.25) is a water level logger. (c) shows the US 101 Slough setup used on June 10, 2020. The green station had 1-minute interval loggers and were used for the head loss analysis. The station within the culvert (STA 1.75) is a water level logger.

Data Processing

Data collected by Onset HOBO data loggers were processed using HOBOWare Pro Version 3.7.20. Conductivity data was converted to salinity using the Conductivity Assistant tool in HOBOWare and using the Non-Linear, Sea Water Compensation based on PSS-78 to determine Temperature Compensation. The water level loggers collected absolute pressure data. The Barometric Compensation Assistant tool in HOBOWare used to atmospheric data to convert the absolute pressure into a water depth. The tool also utilized the reference water level taken during the download to convert the water depth to a water surface elevation in the NAVD88 vertical datum. ADCP discharge and velocity measurements were processed in WinRiver2 software.

Velocity Analysis

ADCP discharge measurements and gate opening geometry were used to calculate the velocity through the gates. ADCP discharge measurements were taken between every 2 and 5 minutes and the data was linearly interpolated between each measurement to assign a discharge value for every minute. This allowed for a discharge measurement that would correspond with each angle measurement. For each angle measurement, the opening area through the gate was calculated based on angle, depth, and tide gate/culvert geometry. For Gannon Slough, the opening area was estimated to include the bottom opening area and both side opening areas. The side opening area included the portion of the triangular opening covered by the water depth within the culvert (Figure 20). The bottom area was calculated by multiplying w (See Figure 20) by the width of the

gate/culvert. At US 101 Slough, the smallest opening area through the gates was used to calculate velocity. The opening area was determined to be w (See Figure 21) by the depth of the water. Velocity through each gate was calculated by dividing the discharge by the opening area at both sites.

$$\text{Opening Area} = 2(\text{Side Opening Area}) + (\text{Bottom Opening Area})$$

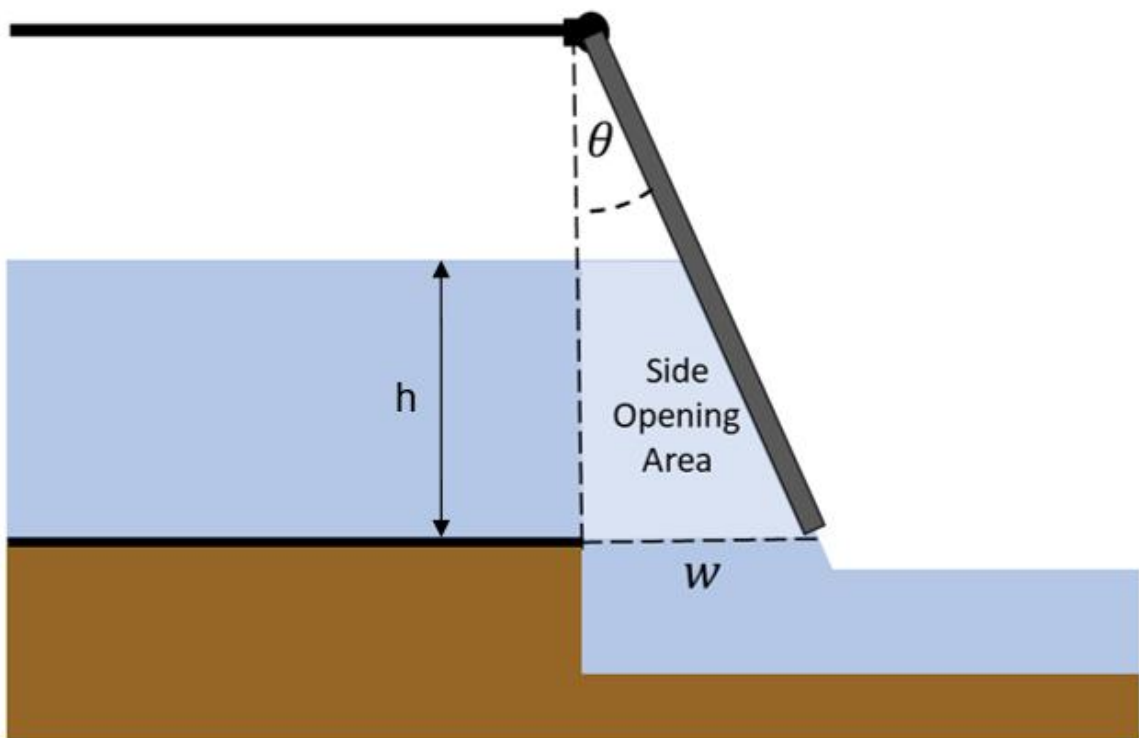


Figure 20. Diagram of profile for top hinged gate at Gannon Slough showing what is considered the opening area. The bottom area is calculated by multiplying w by the width of the culvert.

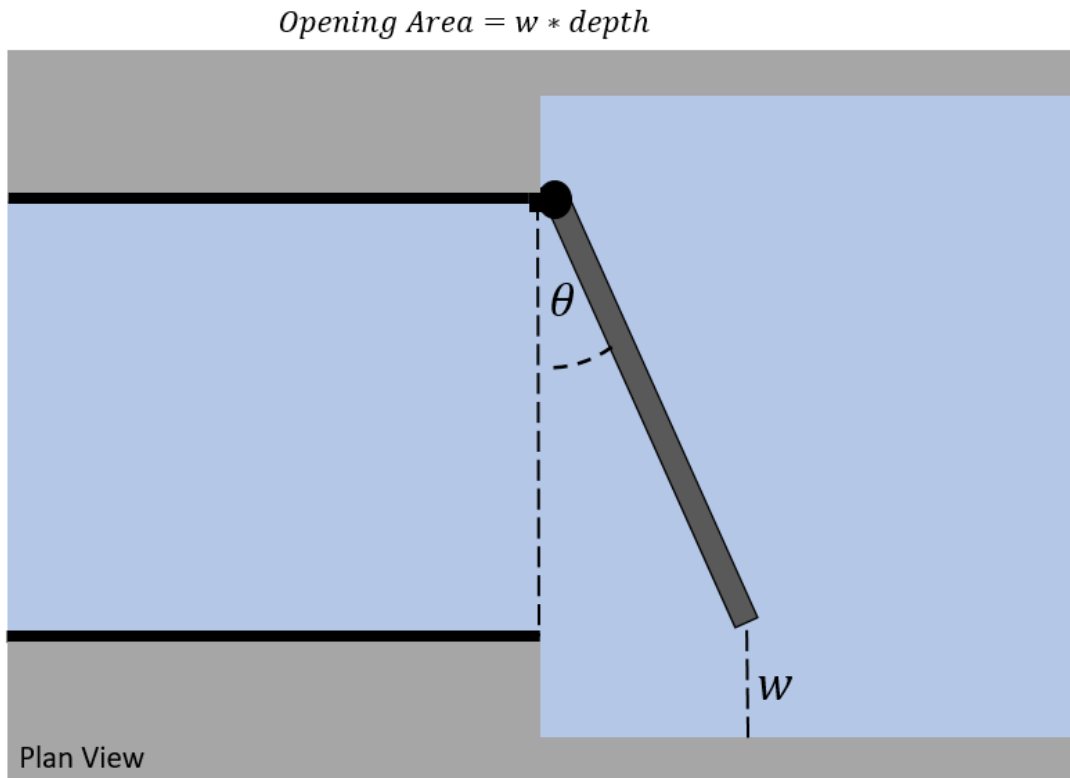


Figure 21. Plan view diagram of side hinged gate at US 101 Slough showing what is considered the opening area.

Gannon Slough discharge measurements were able to be divided into the discharge moving through each of the three gates because the measurements were taken directly upstream of the culverts. During the discharge measurements, the coordinates of the boundary wall between the three culverts were recorded to assist in determining where to split the recorded total discharge measurements. Discharge values related to latitude and longitudinal coordinates throughout the cross-section were exported from WinRiver2. Using the culvert wall locations measured by the ADCP, flow was divided between the three gates for each discharge measurement.

For the US 101 Slough, discharge measurements were collected further upstream of the gate than desired due to interference with vegetation directly upstream of the gate. The distance between the gates and the ADCP measurements did not allow for the culvert locations to be measured along the cross-section. Because the flow distribution was expected to change over the distance, discharge was divided equally between the two gates.

Energy Loss Analysis

An energy loss analysis to determine how the tide gates affected the total energy loss was initially performed using water levels, discharge values and angle measurements. Data collected during the detailed monitoring that occurred on May 18, 2020 at Gannon Slough and June 10, 2020 at US 10 Slough were used to complete this analysis. These two sets of measurements were used because they incorporated additional loggers that measured water level within the culvert. Energy loss estimates were calculated for total loss, entrance loss, friction loss and exit/gate loss. Losses were only calculated during time steps that had a corresponding gate opening angle measurement. This allowed head loss results to be compared to velocity and angle opening to determine if any correlation was present. The methods used to calculate each loss are described in detail below.

Total Head Loss

For this analysis, total head loss was assumed to include entrance head loss, trash rack head loss at US 101 Slough, friction head loss, and tide gate head loss. Each component was calculated separately, except for gate loss which relied on subtracting the other component head loss values from the total head loss. Total head loss for each gate opening angle was calculated using two methods. Method 1 used the channel geometry, and the upstream and downstream water depths to determine total loss (Equation 8a). Method 2 incorporated the same calculation but also accounts for an upstream or approach velocity head (Equation 8b).

$$h_L = d_1 - d_2 + \Delta z \quad (\text{Eq. 8a})$$

$$h_L = d_1 - d_2 + \Delta z + \frac{V_{us}^2}{2g} \quad (\text{Eq. 8b})$$

Where:

h_L	=	Total head loss
d_1	=	Upstream depth
d_2	=	Downstream depth
Δz	=	Difference between upstream and downstream channel bottom elevation
$\frac{V_{us}^2}{2g}$	=	Upstream velocity head

Entrance Head Loss

Entrance head loss was calculated using two methods. Method 1 calculated the head loss from the water surface elevation change between the upstream (Station 1.75 for Gannon and Station 2 for Us 101) and culvert (Station 1.25 for Gannon and Station 1.75 for US 101) stations (See Figure 19). Equation 8a was used with the modification that the culvert station depth was used instead of the downstream station. It was assumed that the upstream velocity head was zero due to the low approach velocities.

Method 2 used average entrance loss coefficients (k_{ent}) for culverts with multiple barrels that were presented in Jones et al. (2006). Culverts that were most similar to each tide gate system were chosen and are shown in Figure 22. Culvert A represented US 101 Slough and had an average entrance loss coefficient of 0.57. Characteristics of Culvert A include 0-degree wingwalls, 4-inch straight top bevel, extended center walls, and 6-inch corner fillets. This deviated from the actual US 101 culvert because it did not have a top bevel or corner fillets. Culvert B represented Gannon Slough and had an average entrance loss coefficient of 0.46. Characteristics of Culvert B include 30-degree flared wingwalls, and 4-inch straight top bevel. Additionally, Culvert B was at a 45-degree skew from the channel. This deviated from the actual Gannon culvert because the Gannon Slough culverts do not have a top bevel or the flared wingwalls. Additionally, the Gannon Slough culverts are at an approximately 90-degree skew from the upstream channel. The average entrance head loss coefficients from Jones et al. (2006) were used to calculate the entrance head loss and used the velocity within the culvert (Equation 9). Equation 9 is an

equation that can be utilized to determine the head loss values of different components depending on the head loss coefficient that is used.

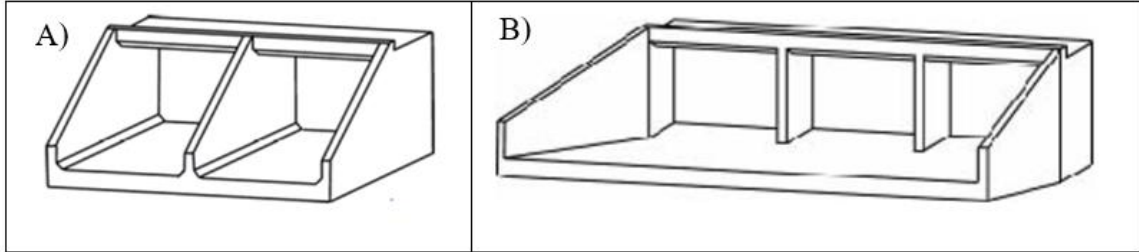


Figure 22. Culvert configurations from Jones et al. (2006). US 101 Slough used Culvert A's entrance loss coefficient and Gannon Slough used Culvert B's entrance loss coefficient. Figures adopted from Jones et al. (2006).

$$H_{loss} = k_{loss} \frac{V^2}{2g} \quad (\text{Eq. 9})$$

Where:

H_{loss} = Head loss (total, entrance, gate, etc.)

k_{loss} = Head loss coefficient (total, entrance, gate, etc.)

V = Velocity

Friction Head Loss

Friction head loss was calculated using the Manning's Darcy Equation (Equation 10) and Haaland and Darcy Equations (Equations 11 and 12).

$$h_f = \frac{29n^2 L V^2}{R_h^{1.33} 2g} \quad (\text{Eq. 10})$$

$$f = \left(\frac{1}{-1.8 \log_{10} \left[\left(\frac{\epsilon/D_H}{3.7} \right)^{1.11} + \frac{6.9}{Re} \right]} \right)^2 \quad (\text{Eq. 11})$$

$$h_f = f \frac{L}{4R_h} \frac{V^2}{2g} \quad (\text{Eq. 12})$$

Where:

h_f	=	Friction head loss
n	=	Mannings's roughness coefficient (0.013)
L	=	length of culvert
V	=	Culvert velocity
R_h	=	Hydraulic radius
f	=	Darcy friction factor
ϵ	=	Relative roughness (5.83×10^{-4} ft)
D_h	=	Hydraulic diameter
Re	=	Reynolds number

Tide Gate/Exit Head Loss

The tide gate/exit loss was also calculated using two methods. Method 1 used the total head loss and subtracted entrance loss and friction loss to determine the gate/exit loss. For this method, the Method 1 entrance loss was used because it was the larger loss and relied on actual data collected on site.

Method 2 for calculating the gate/exit loss used the difference between the water surface elevations between the culvert station and the downstream station (see Equation 8a); thus, isolating the gate hydraulics and losses.

Discharge Coefficient

Gannon Slough has a perched outlet between the downstream slough and the gate/culvert system. Due to the elevation drop and the top-hinged gates not being able to open until the tidal side (downstream) water surface elevation is near the culvert bottom, the tide gate acts as a free jet during a majority of the gate opening time. Because of this, a tide gate head loss coefficient was not able to be calculated. A tide gate discharge coefficient was instead calculated to further help establish hydraulic parameters for tradition tide gates. Discharge coefficients are a ratio between the actual discharge and theoretical discharge and are common hydraulic parameters used within modeling software. At Gannon Slough, discharge coefficients based on the opening area through the gate (see Figure 20) were calculated (Equation 13). Discharge coefficients were then compared to angle measurements and discharge to determine how they varied throughout the gate opening.

$$C_d = \frac{Q}{A\sqrt{2gh}} \quad (\text{Eq. 13})$$

Where:

C_d = discharge coefficient

Q = flow rate

g = gravitational acceleration constant

h = upstream water depth

RESULTS

This section presents results from analysis of the traditional, top-hinged gate system at Gannon Slough and the aluminum, side-hinged gate system located at US 101 Slough. This study was mainly interested in determining head loss coefficients for each gates type. Due to the configuration of Gannon Slough, tide gate head loss coefficients were not able to be calculated, and discharge coefficients, another common hydraulic parameter used in hydraulic models, were calculated for this site.

For both sites, various head losses throughout the entire structure were calculated. At Gannon Slough, friction and entrance head loss were determined. Total and tide gate head loss where not able to be calculated due to the open jet behavior at the gates. At US 101 Slough, total, friction, entrance and gate loss were calculated. Each head loss component was calculated multiple ways as described in the Methods section.

Gannon Slough

As previously stated, head loss components were calculated various ways to determine what was most appropriate for each site. For Gannon Slough, total head loss was calculated using Method 1 due to the small percent difference between the results from both methods and minimal upstream velocity. Entrance loss was calculated using Method 1, which calculated the head loss between Stations 1.75 and 1.25 using the Bernoulli Equation and was assumed to be more accurate because it used site-specific measurements. Method 2 may have produced smaller results due to differences in

geometry between Gannon Slough culverts and the culverts studied by Jones et al. (2016) and a larger skew (approximately 90 degrees) of the upstream channel entering the culverts. Friction loss was calculated using one method, and used the Darcy-Weisbach equation and the Manning's equation to calculate the friction coefficient (f).

Gannon Slough had three traditional, top-hinged gates prior to replacement in September 2020. The following results are based on velocity and discharge measurements made using the ADCP on May 18, 2020. The ADCP setup at Gannon Slough was directly upstream of the culverts/tide gates, which allowed for the discharge measurements to be divided between the three culverts based on measurement location (See Methods section). Figure 23 shows the flow distribution through each culvert over time.

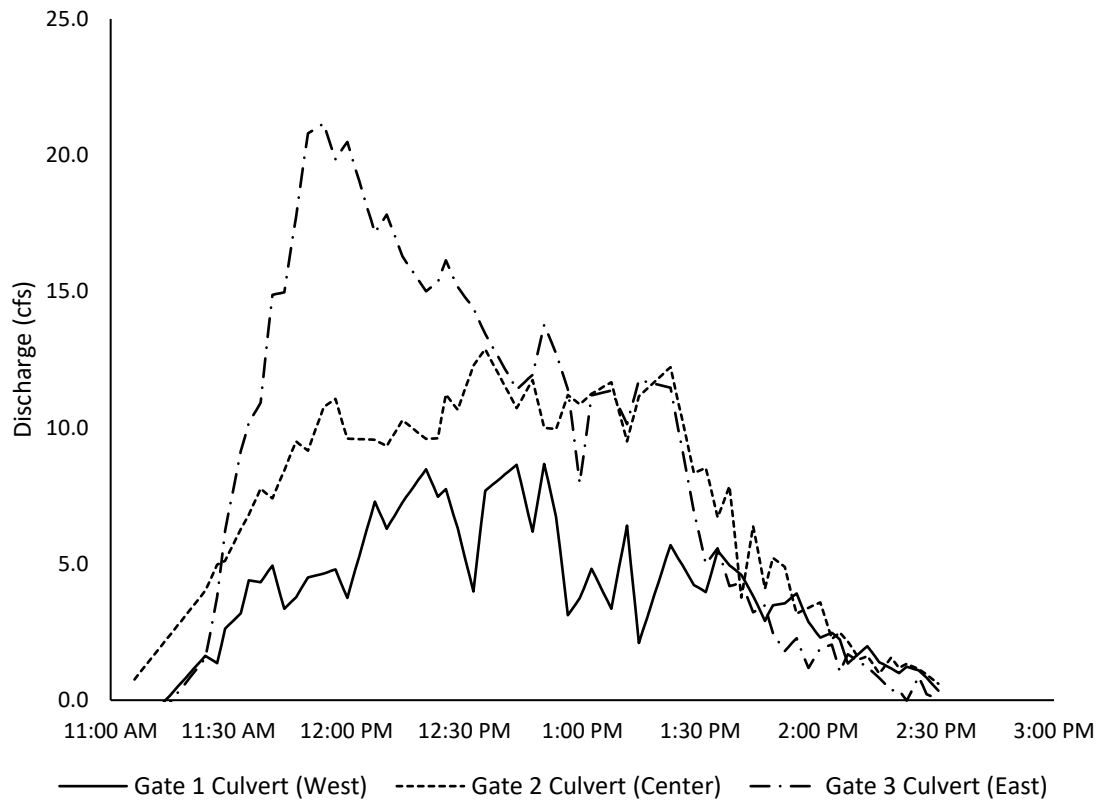


Figure 23. Plot showing discharge versus time entering each culvert at Gannon Slough during ADCP measurements taken on May 18, 2020.

The Gannon Slough tide gate system has a perched outlet above the downstream channel that is approximately 1.5 feet above the downstream channel bottom. The weight of the large gate limited the gate opening to small angles (the largest angle recorded being 6.3 degrees) that were only achieved when the downstream water surface was near or below the culvert outlet invert. This condition resulted in tide gate outflow similar to a free jet. For this case, head loss could not be calculated using measured upstream and downstream station elevations. Due to this behavior, discharge coefficients for a free-jet,

orifice flow were calculated for Gannon Slough. Figure 24 and Figure 25 show discharge coefficients compared to discharge through each culvert and gate opening angle.

Gate 1 and Gate 2 each had one discharge coefficient value calculated to be above 1 and these were considered outliers because a discharge coefficient cannot be greater than 1. Both outliers occurred during the closing of the gates and when the gate angle openings were 0.5 degrees at Gate 1 and 0.3 degrees at Gate 2. was below 1 degree. The small openings at each gate would have caused high velocities that would lead to higher discharge coefficients.

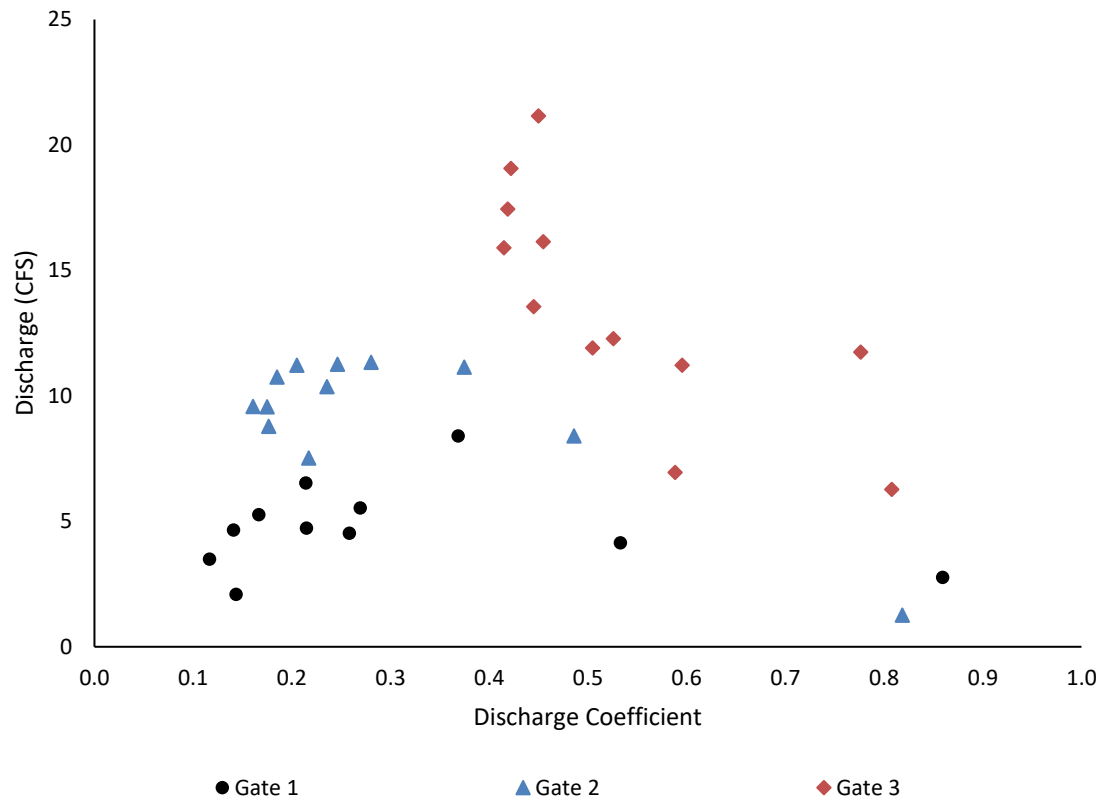


Figure 24. Discharge coefficient versus discharge for Gannon Slough measurements taken on May 18, 2020. Gate 1 and Gate 2 had discharge coefficients greater than 1 that occurred when the angle opening was below 0.5 degrees. Outliers are not shown.

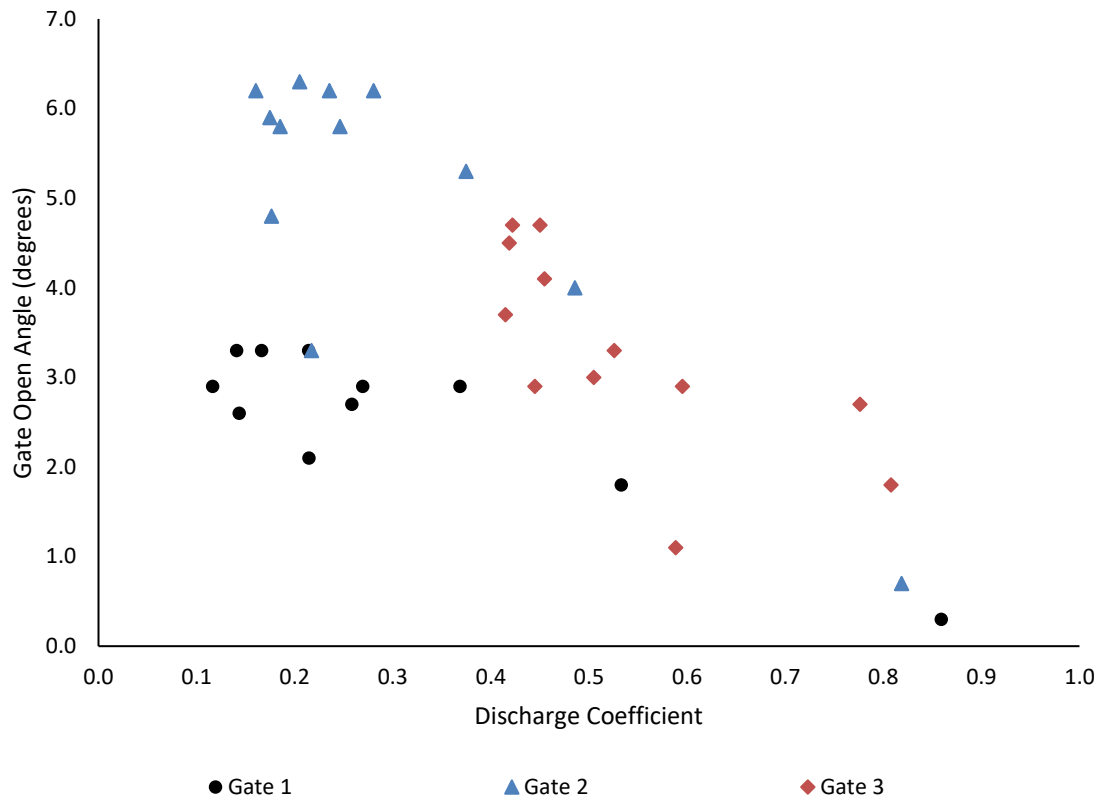


Figure 25. Discharge coefficient versus gate angle opening for Gannon Slough measurements taken on May 18, 2020. Gate 1 and Gate 2 had discharge coefficients greater than 1 that occurred when the angle opening was below 0.5 degrees. Outliers are not shown.

Table 9 summarizes the discharge coefficient statistics for each gate excluding the outliers. Gate 1 had the largest discharge coefficient range between 0.12 and 0.86 and had a standard deviation of 0.22. Gate 2 discharge coefficients ranged between 0.16 and 0.82 with a standard deviation of 0.19. Gate 3 had the smallest range, 0.42 and 0.81, with a standard deviation of 0.14. However, Gate 3 opening angles were only recorded for the first two hours of the three-hour measurement period. Gate 1 and Gate 2 each had their maximum discharge coefficient after Gate 3 angle measurements had stopped.

Table 9. Summary of basic statistics regarding the discharge coefficient of each gate at Gannon Slough.

	Gate 1	Gate 2	Gate 3
Maximum Discharge Coefficient	0.86	0.82	0.81
Minimum Discharge Coefficient	0.12	0.16	0.42
Average Discharge Coefficient	0.30	0.30	0.53
Standard Deviation	0.22	0.19	0.14

Though the tide gate head loss was not able to be calculated due to the perched outlet and open jet behavior, head loss values were calculated for the entrance and friction within the culvert. The entrance loss values ranged between 0.00 feet and 0.07 feet and the friction loss values ranged between 3.6×10^{-5} feet and 8.3×10^{-3} feet. All the calculated head loss values can be found in Appendix B.

US 101 Slough

For US 101 Slough, total head loss was calculated using Method 1, which neglected the approach velocity head. This method was the preferred option due to the small percent difference between the results from both methods and minimal upstream velocity at both sites. For the entrance loss, Method 1 produced results that were much larger than Method 2 and resulted in an average percent difference of 191 percent. It was assumed that the actual entrance loss due to the culvert at US 101 Slough would be better approximated by Method 2 because it calculated entrance head loss based on previously studied multi-barrel culverts similar to US 101 Slough. However, Method 1 was more accurate at calculating the head loss between Station 2 and Station 1.75. The difference in

results between the two methods was assumed to be from the trash rack directly upstream of the culvert that was blocked by debris during measurements. Due to the presence of the debris, it was assumed that the difference between the results from both methods was head loss due to the trash rack. Friction head loss was calculated using the Darcy-Weisbach equation and the Manning's equation to calculate the friction coefficient (f).

The US 101 Slough has two aluminum, side-hinged gates with a small permanent opening located on the east door. The ADCP measured discharge approximately 250 feet upstream of the gates on June 10, 2020. Figure 26 shows the velocity through the tide gates and total discharge at US 101 Slough during the gate opening. Figure 27 and Figure 28 show various components of the system's head loss and total discharge over time. Each plot includes total head loss, entrance loss, trash rack loss, friction loss and exit/tide gate loss. These figures are based on times when in-field angle measurements were taken. Gate 2 had a rapid, instantaneous gate closing phase that did not allow for any angle measurements to be taken. Additionally, measurements were not taken when there were no visible changes in angle and resulted in a shorter data set.

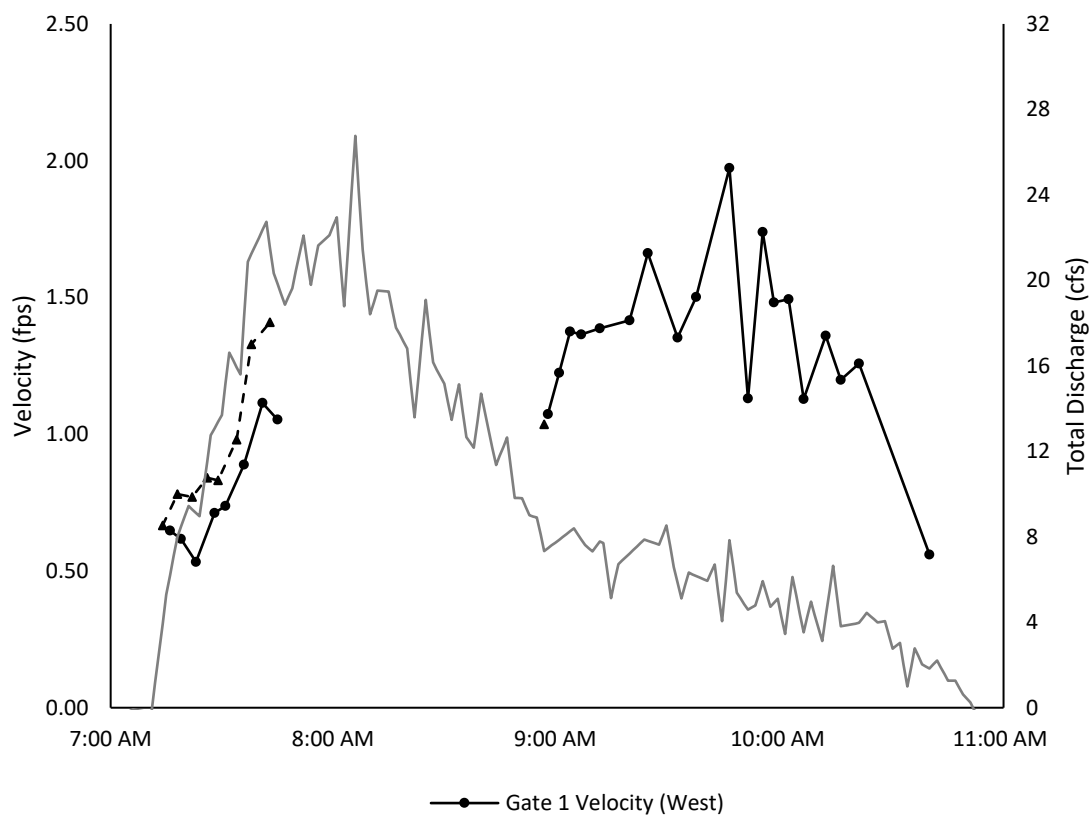


Figure 26. Average velocity through the gate openings and total discharge for US 101 Slough. Velocity measurements correspond to when in-field angle measurements were taken.

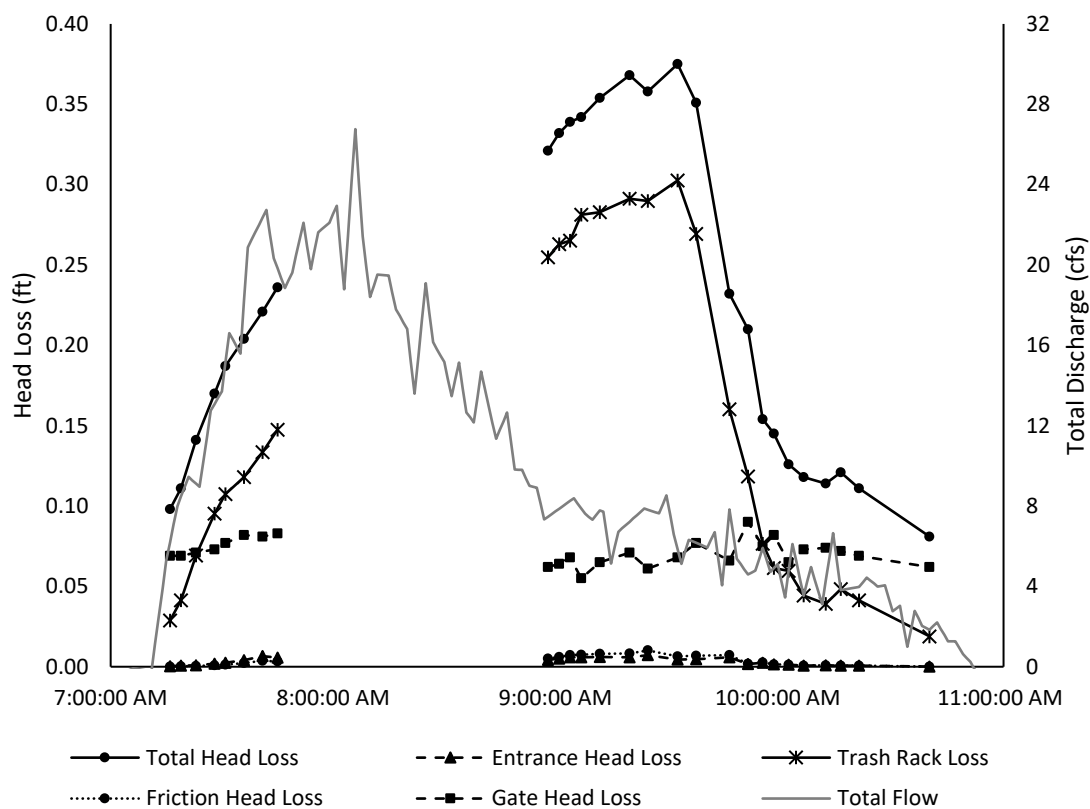


Figure 27. Total head loss and head loss components at US 101 Slough's Gate 1 based on measurements performed on June 10th, 2020. Head loss comprised of entrance loss, trash rack loss, friction loss and gate loss.

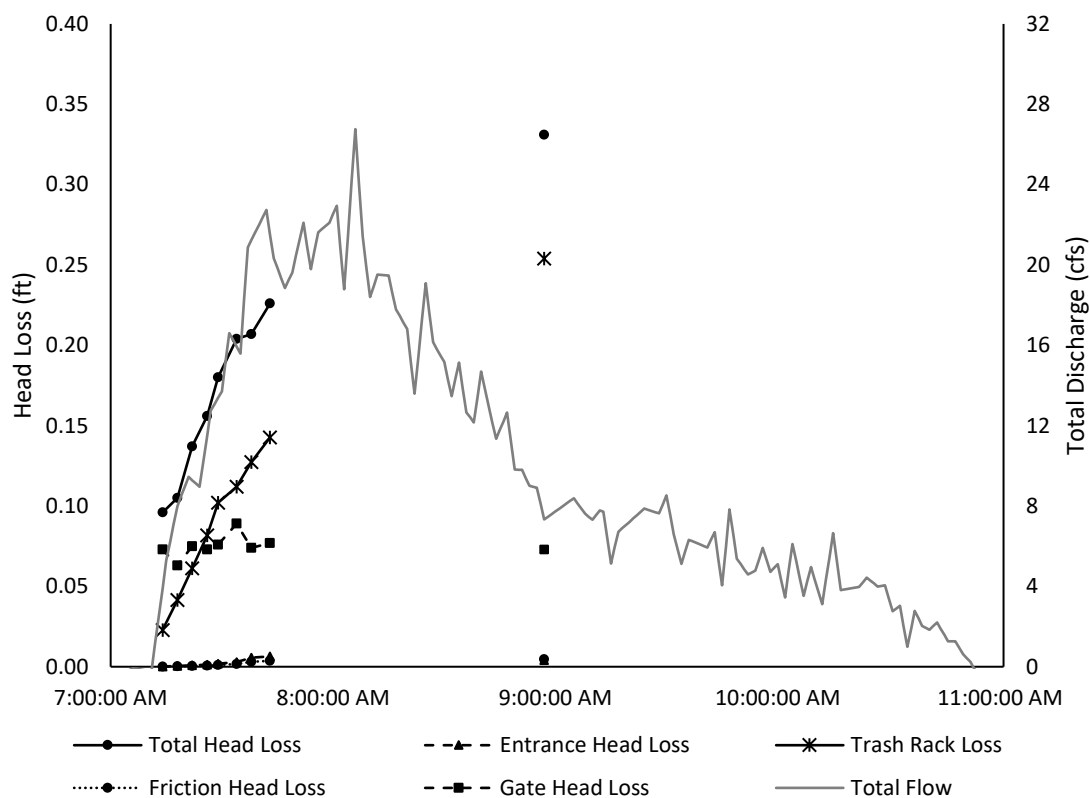


Figure 28. Total head loss and head loss components at US 101 Slough's Gate 2 based on measurements taken on June 10th, 2020. Head loss comprised of entrance loss, trash rack loss, friction loss and gate loss.

The entrance, friction and gate loss were relatively constant throughout the gate opening event, while the trash rack loss varied with discharge and velocity rates. The gate loss results were analyzed in more detail and are presented below.

Head loss attributed to just the side-hinged tide gate had little variation throughout the measurement event. Gate 1 had an average head loss of 0.071 feet and Gate 2 had an average head loss of 0.075 feet over a total discharge range through both gates measured between 0.249 cfs and 26.76 cfs. Table 10 shows the statistics of the gate

head loss values. Gate 1 had a tide gate head loss ranging between 0.055 feet and 0.090 feet with a standard deviation of 0.008 feet. Gate 2 had a tide gate head loss ranging between 0.063 feet and 0.075 feet with a standard deviation of 0.009 feet.

Table 10. Statistics of tide gate head loss values for Gate 1 and Gate 2 at US 101 Slough. Values were based on measurements taken in the field on June 10th, 2020.

	Gate 1	Gate 2
Maximum Head Loss(ft)	0.090	0.075
Minimum Head Loss (ft)	0.055	0.063
Average Head Loss (ft)	0.071	0.075
Standard Deviation (ft)	0.008	0.007

Using the gate head loss values, gate head loss coefficients were calculated using a rearranged form of Equation 9. Average velocity through each gate opening was used to calculate the coefficients. Gate loss coefficients were divided into three phases: gate opening, gate fully open and gate closing. Table 11 shows the tide gate loss coefficient statistics for each gate and phase.

Table 11. Tide gate coefficient values for US 101 Slough Gate 1. Angle range was based only on angles measured by hand.

	Gate Opening	Gate Fully Open	Gate Closing
Angle Range (degrees)	34.6 – 59.8	66.0 – 68.5	21.3 – 58.0
Maximum Coefficient	16.07	9.27	12.74
Minimum Coefficient	9.27	4.20	1.09
Average Coefficient	11.89	6.20	3.02
Standard Deviation	2.95	2.21	2.49

Table 12. Tide gate coefficient values for US 101 Slough Gate 2. Angle range was based only on angles measured by hand. Gate 2 closed almost instantaneously, preventing any measurement during the Gate Closing phase.

	Gate Opening	Gate Fully Open	Gate Closing
Angle Range (degrees)	20.0 – 48.2	55.0 – 58.2	-
Maximum Coefficient	10.58	7.07	-
Minimum Coefficient	6.65	2.50	-
Average Coefficient	8.00	4.52	-
Standard Deviation	1.86	2.00	-

Discharge Coefficient

In addition to calculating tide gate head loss coefficients for US 101 Slough, discharge coefficients for the tide gates were estimated using the method outlined in Cassan et al. (2018). This method was utilized because they were both side-hinged gate. However, the Cassan et al. (2018) study was modeling the closing of the gate and labeled the upstream channel as the tidal channel and the downstream channel as the freshwater channel. For US 101 Slough, the upstream channel was the freshwater channel, and the downstream channel was the tidal channel. Equation 3 was used to calculate the discharge coefficient. The contraction coefficient and downstream Coriolis coefficient

values were taken for the Cassan et al. (2018) study and had a value of 0.75 and 1.05, respectively. The results were then overlayed onto plots produced by Cassan et al. (2018) and can be seen in Figure 29.

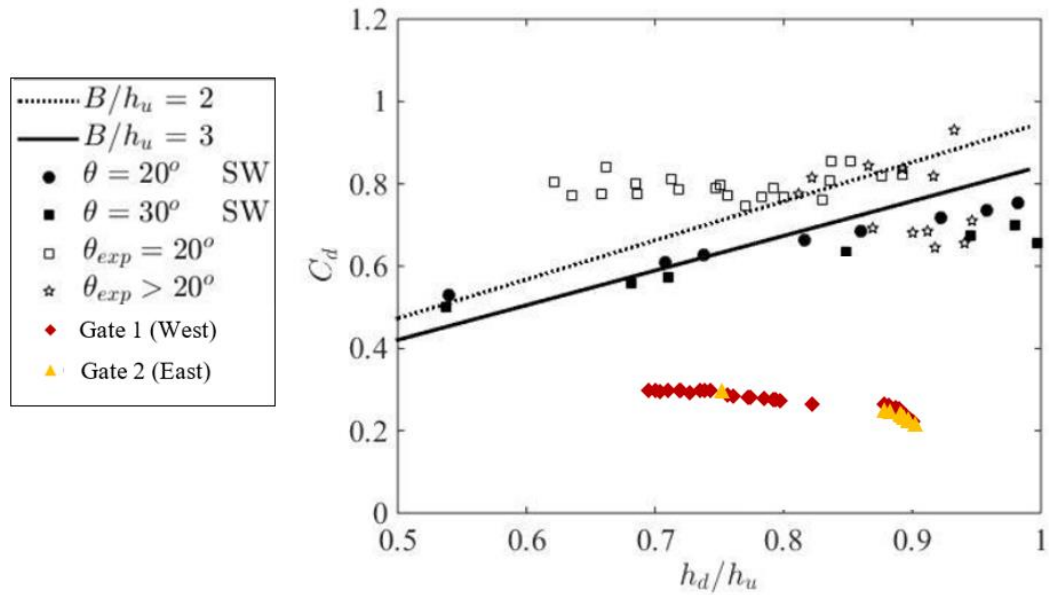


Figure 29. Water depth ratio versus tide gate discharge coefficient results from Cassan et al. (2018) and US 101 Slough that was calculated using the same method as Cassan et al. (2018). Figure adapted from Cassan et al. (2018).

Fish Passage

Angle measurements taken during the ADCP measurements were used to calculate the average velocity through the gates for both Gannon Slough and US 101 Slough. The velocities through the gates were assumed to be the fastest velocities within the system because the gate opening area is smaller than all other system components. These values were compared to fish passage criteria for juvenile and adult salmonids to determine the duration of passable conditions (CDFG 2004 and NMFS 2001).

Gannon Slough velocity results compared to maximum average velocity for juvenile and adult salmonids are shown in Figure 30. Based on velocity values calculated through the gate openings, velocity criteria were not met for juvenile salmonid passage at any time during the gate opening. Gate 1 met velocity criteria 83 percent of the time that gate angle openings were measured for adult anadromous and non-anadromous salmonids. Gate 2 met velocity criteria 92 percent of the time for adult anadromous and non-anadromous salmonids. Gate 3 was 83 percent passable for adult anadromous salmonids and zero percent passable for non-anadromous salmonids.

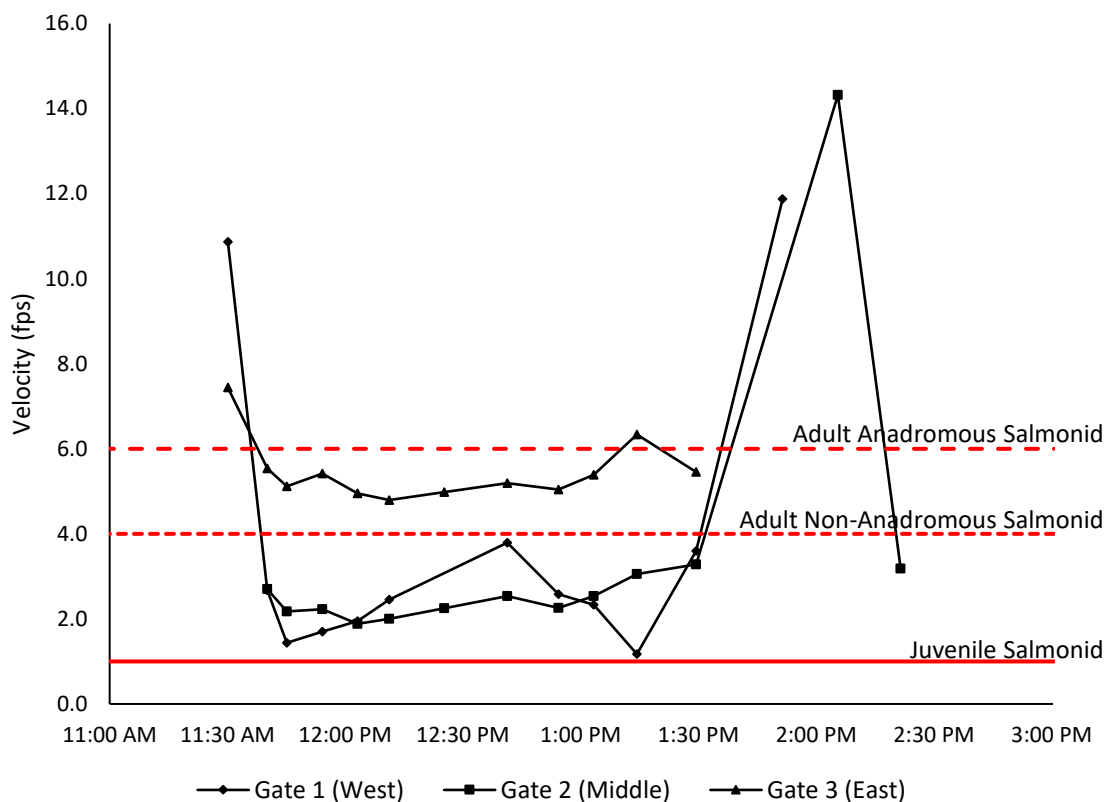


Figure 30. Average velocities through each Gannon Slough gate compared to fish passage velocity criteria for juvenile and adult salmonids (CDFG 2004).

Figure 31 shows average velocity through the gates at US 101 Slough compared to velocity criteria for juvenile and adult salmonids (CDFG 2004). Both gates met velocity criteria 100 percent of the time for adult anadromous and non-anadromous salmonids. The juvenile salmonid velocity criteria were met 26% of the time at Gate 1 and 67% of the time at Gate 2 based on times when angle measurements were taken. However, Gate 1 had more measurements throughout the gates opening cycle, so Gate 2

may have a percent time passable more similar to Gate 1 since the velocities that exceeded the criteria were measured after Gate 2 was no longer being measured.

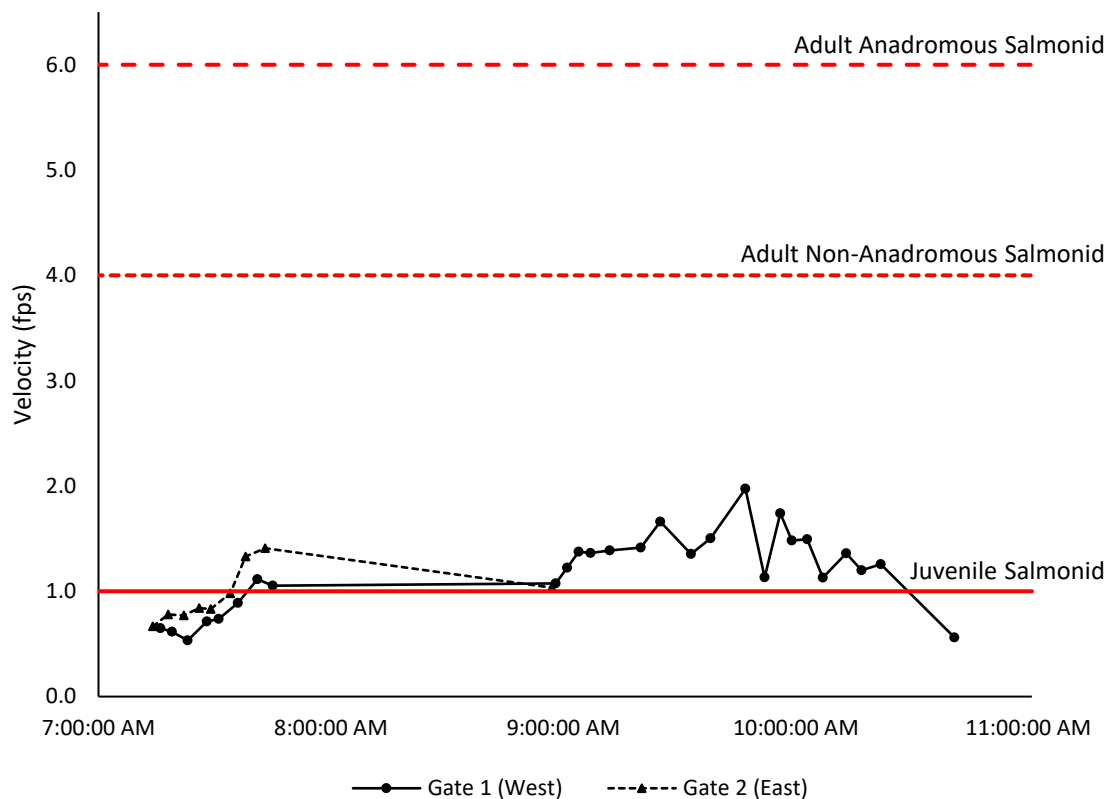


Figure 31. Average velocities through the US 101 Slough tide gates compared to the fish passage velocity criteria for juvenile and adult salmonids (CDFG 2004).

DISCUSSION

The following section describes the discharge coefficients and head loss coefficients identified for the tide gate hydraulics observed at both Gannon Slough and US 101 Slough. Due to the open-air jet created by the perched outlet and the weight of the traditional gates, the Gannon Slough culverts and tide gate head losses could not be calculated from water elevation data. Instead, discharge coefficients for an open-air jet were calculated at Gannon based on the opening area (see Figure 20). The Cassan et al. (2018) study calculated discharge coefficients for side-hinged tide gates. Their method was not applicable to the Gannon Slough site because of the different gate configuration and Gannon Slough had a free outfall.

US 101 Slough used water elevation changes measured through the culvert and tide gate structure to determine head loss through each tide gate. Gate opening angle measurements were used to determine the velocity through the gate and calculate head loss coefficients for each gate.

Gannon Slough

At Gannon Slough, discharge coefficients for a free jet outlet were calculated for each tide gate based on the velocity through the gate opening. Figure 25 shows that Gate 2 had the largest measured gate opening angle. As the gate opening angle increased, the discharge coefficient decreased. Though Gate 2 had the largest gate opening angles,

ranging between 0.3 and 6.3 degrees, Gate 3 had the overall largest maximum discharge value of 21.16 cfs, followed by Gate 2 with 12.88 cfs and Gate 3 with 8.67 cfs.

Excluding the outliers estimated during the gate closure, all other discharge coefficient estimates were below 1. Linear trend lines were applied to Figure 25, but had low R^2 values (< 0.78) when comparing angle opening or discharge. Based on visual inspection, the discharge coefficients for all of the gates had a linear trend that decreased as the angle increased. This observation may have been influenced by the limited data values and additional data could alter the results. A trend was not as apparent when comparing the discharge coefficient to discharge. However, the outliers only occurred during low discharges (less than 5 cfs) and small gate opening angles (less than 1 degree).

Gate 1 and Gate 2 had the same average discharge coefficient of 0.30. Additionally, they had similar discharge coefficient ranges and standard deviations (Table 9). Gate 3 produced a larger average discharge coefficient, 0.53, and had a small range of discharge coefficient values. As previously stated, Gate 3 did not have measurements taken throughout the entire gate opening cycle and may not provide a comprehensive range of values. However, within the period when Gate 3 measurements were taken, Gate 1 and Gate 2 still had a lower average discharge coefficient (0.30 for Gate 1 and 0.25 for Gate 2) than Gate 3. One noticeable difference between Gate 3 and the other two gates was that Gate 3 had a larger discharge during a majority of the opening.

A discharge coefficient of 0.38 is recommended when modeling a small-scale, traditional, top-hinged gate based on the above results. This value is an average of all the

calculated discharge coefficients excluding the two outliers. This value would be most accurate when the gates were fully open and discharge was at its peak. During the opening and closing of the gates larger discharge coefficients were observed. For the Gannon Slough site, the opening of the gates occurred at a faster rate than the closing. The extended closing time resulted in discharge coefficients that ranged between 0.49 and 0.819 between all three gates and included two discharge coefficients outliers above 1. The opening phases had discharge coefficients that ranged between 0.18 and 0.86 but did not have any discharge coefficients above 1. The large discharge coefficients during the opening and closing of the Gannon Slough gates were related to small angle measurements. The traditional gates were old and did not completely close due to decaying hinges. This may have resulted in flow through the gates even when the head differential would have not been able to open the gates.

US 101 Slough

Head loss analysis for the two gates at US 101 Slough was divided into three phases based on gate opening angle: gate opening, gate fully open, and gate closing. The opening phase of the US 101 Slough gates took approximately 15 minutes before gates reached fully open. The average fully open phase angle was 68 degrees for Gate 1 and 58 degrees for Gate 2. The fully open phase for Gate 1 lasted approximately 1.5 hours. Gate 1 had a gradual closing phase that lasted for approximately an hour and forty-five minutes. Gate 2 did not have any measurements taken during its closing phase due to it rapidly shut over a few seconds. Gate 2 was fully open for approximately four hours.

The tide gate head loss was fairly constant throughout the whole gate opening phase and had an average value of 0.071 feet for Gate 1 and 0.075 feet for Gate 2 (Table 10). Tide gate head loss at the US 101 Slough made up 16 to 77 percent of the total head loss through the tide gate structure during the gate opening phase. However, the trash rack head loss varied the most out of each component and ranged between 3-5 times larger than the other head loss components during the fully open phase.

Tide gate head loss coefficients were calculated based on velocity through the gate opening area. For both gates, the opening phase resulted in the largest average head loss coefficient (11.89 for Gate 1 and 8.00 for Gate 2). The high head loss coefficients during the opening phase were mainly due to gate velocities below 1 fps that increased the head loss coefficient value based on Equation 9. For Gate 1, the fully open phase had the next highest head loss coefficients with an average head loss coefficient of 6.20. Head loss coefficients during the fully open phases decreased with time over the gate opening cycle with larger head loss coefficients at the beginning of the phase due to velocities below 1 fps caused by the greater water depths within the culvert. The closing phase had the lowest head loss coefficients with an average of 3.02. During the closing phase the gate had velocity measurements above 1 fps, except the last measurement with a velocity of 0.56 fps. This low velocity value caused the last measurement at Gate 1 to have a head loss coefficient of 12.74, while the rest of the phase had head loss coefficients that ranged between 1.09 and 4.53.

The average head loss coefficient during the fully open phase of Gate 2 was 4.52 and was smaller than Gate 1. Gate 2's fully open phase was measured for the same

amount of time as Gate 1's fully open phase (approximately 1.5 hours). The gate was open for an additional 2.5 hours after the last measurement, but additional measurements were not collected because the gate opening angle did not change. Gate 2 had a fully open gate angle that was on average 10 degrees smaller than Gate 1. The smaller flow area of Gate 2 resulted in higher velocities and, therefore, a smaller head loss coefficient. As stated above, Gate 2 did not have measurements during its closing phase, so its performance during this phase could not be compared to Gate 1.

For modeling a side-hinged tide gate similar to US 101, a head loss coefficient of 5.27 is recommended to produce the most accurate overall results. This value is based on the average head loss coefficients for the fully open phase for both gates. The large gate loss coefficient at the closing of Gate 1 was omitted. The fully opened phases were used in the final average because it incorporated lower velocities that resulted in high head loss coefficients that would be present in a similar system. The closing phase for Gate 1 had the longest time period (approximately one hour and forty-five minutes). However, it was not included due to Gate 2 not having a closing phase.

Discharge Coefficient Discussion

The discharge coefficients results for US 101 Slough were compared to the discharge coefficient experimental results (white square and star markers) from Cassan et al. (2018). US 101 Slough values ranged between 0.208 and 0.291, while Cassan's results based on visual inspection ranged between 0.6 and 0.9. Cassan's results were based on angle opening measurements between 20 and 30 degrees. The discharge coefficients

related to the 20-degree angle openings were overall larger than the discharge coefficients related to the 30-degree angle openings and averaged around 0.8. The discharge coefficients related to the 30-degree angle openings had a large range, but usually had a smaller discharge coefficient when compared to the 20-degree opening discharge coefficients at similar water depth ratios. The decrease in discharge coefficients as the angle increased could potentially explain why the US 101 Slough, which had angle openings ranging between 20 and 68.5 degrees and an average angle opening of 46.4 degrees. However, this does not explain why the smaller angles at US 101 Slough did not have larger discharge coefficients. This could be explained by the contraction coefficient and Coriolis coefficient being derived for the Cassan gate, and may need to be adjusted to better represent US 101 Slough.

Fish Passage Criteria

Fish passage criteria for tide gates are under development in California, but there are currently not any published criteria. Many tide gate improvement projects use fish passage criteria related to river restoration. Both sites are salmonid and tidewater goby habitat. Thus, each site was evaluated using salmonid passage criteria from California Department of Fish and Wildlife (CDFG 2004). There are currently no official criteria for tidewater goby.

US 101 Slough was able to provide better passage for both adult and juvenile salmonids than Gannon Slough based on velocity criteria. US 101 Slough met velocity criteria for adult salmonids throughout the entire gate opening. The juvenile salmonid

velocity criteria were only met at US 101 Slough during the opening and the closing phases of the gate when the velocities were below 1 fps. However, the velocities compared to the passage criteria are at the gate opening where velocities are expected to be the highest due to the smallest cross-sectional area. Once through the gate opening constriction, velocities within the culvert were all below 1 fps for the entire gate opening cycle.

Gannon Slough was not able to meet velocity criteria for juvenile salmonid passage at any point during the gate opening cycle. Velocity criteria were met on average between the three gates 86 percent of the opening time for adult anadromous and non-anadromous salmonids. Velocities above the adult passage criteria occurred during the opening and closing of the gates. Though velocity criteria were partially met during the opening, the gates' largest angle opening was 6.3 degrees at Gate 2. This resulted in a small opening area that may not provide passage for adult salmonids for reasons other than velocity. Additionally, a perched outlet is present downstream of each of the three gates and may hinder passage between the gates and the downstream channel.

RECOMMENDATIONS AND CONCLUSIONS

Recommendations

The following section recommends modifications or additions that could be implemented for field measurements at each site. These recommendations would improve data collection efforts and address data gaps allowing additional verification and understanding of tide gate hydraulics.

Gannon Slough

Gannon Slough had noticeable variation in flow distribution between each of the three culverts. Although ADCP discharge measurements were divided between each culvert, a single water depth logger was placed in the center culvert. To further improve hydraulic measurements within the culvert and through the individual gates, additional water level loggers could be placed in each culvert during ADCP measurements.

Data collection at traditional, multi-gate tide gate sites could be improved upon by taking more gate opening angle measurements throughout the opening and evenly among each gate. Because traditional tide gates tend to have small angle openings (< 10 degrees), frequent and accurate measurements are required to determine their impact on the discharge coefficients and head loss results.

Only one tide gate opening event was measured. Additional measurements during various flow events may result in larger openings and improve the estimation of discharge coefficients. As previously stated, the tilt sensors are not accurate enough to

measure the small angle changes present at these gates. However, the site allowed access to the top of the gates near the hinges even during larger flow events when measuring within the channel is not feasible.

US 101 Slough

US 101 Slough's ADCP measurements were taken approximately 525 feet upstream of the culvert/tide gates. Because they were not taken directly upstream of the culverts, the flow was not able to be divided based on the GPS location of the culvert walls. Thus, it was assumed that flow was divided equally between both culverts. This was justified based on the straight upstream channel alignment, uniform upstream cross-section and physical observation during discharge measurements. Flow distribution between each culvert could be better captured if the ADCP measurements were able to be taken closer to the culvert. However, this may not be possible at this location due to eel grass along the channel that interferes with the ADCP measurements.

Similar to Gannon Slough, only one water level logger was placed in one culvert during the detailed velocity measurements. An additional water level logger in the other culvert would allow for verification of flow and head loss variation throughout the two gates.

US 101 Slough has a trash rack placed upstream of the culvert. During the time of the ADCP measurements, a large amount of debris was caught on the trash rack. The head loss analysis for US 101 showed that the loss between the upstream station (Station 2) and the downstream station (Station 1.75) had the largest loss out of each tide gate

structure component calculated. For the above analysis, the trash rack loss and culvert entrance loss were grouped together. To better distinguish between these contributions to the total head loss, additional water level loggers directly upstream and downstream of the trash rack could better determine how the trash rack head loss impacts the total loss and better differentiate the culvert entrance and tide gate head loss.

US 101 Slough would also benefit from more frequent gate opening angle measurements. The US 101 Slough gates opened to large enough angles that the tilt sensors can accurately measure the gate opening angles. More frequent angle measurements at 1-minute intervals instead of every 15 minutes would better define how the head loss coefficient changes as a function of discharge, gate velocity and upstream depth. Additionally, game cameras could be utilized to film the gate opening. A reference marker could be determined prior to the opening of interest and angle measurements could be derived from the video.

Conclusions

Throughout California, traditional tide gates are currently being replaced by “fish-friendly” tide gates where potential habitat exists. The traditional, top-hinged tide gates at Gannon Slough were compared to the newly replaced “fish-friendly”, side-hinged tide gates. Though there are currently no fish passage criteria specifically for tide gates, each gate type was compared to fish passage criteria for salmonids at stream crossings in riverine systems. The “fish-friendly”, side-hinged gates were able to provide greater passage for adult and juvenile salmonids throughout their opening. Both side-hinged

gates were able to pass adult salmonids 100 percent of the opening. The traditional, top-hinged gates partially met velocity criteria requirements for adult salmonids. Gate 1 and Gate 2 provided passage 83 and 92 percent of the opening time respectively for adult anadromous and non-anadromous salmonids. Gate 3 allowed for adult anadromous salmonid passage 83 percent of the time, but did not meet requirements for adult non-anadromous salmonids during the opening. However, they had small opening area throughout the entire opening period and could potentially hinder passage even when velocity criteria were achieved.

Monitoring each tide gate resulted in calculating discharge coefficients for Gannon Slough and head loss coefficients for US 101 Slough. Though the objective of this thesis was to determine how hydraulic coefficients changed throughout the tide gate openings, evident patterns related to opening and flow were not able to be identified. However, the study was able to identify ranges of applicable values that could be applied to hydraulic models regarding both traditional and side-hinged gates. Discharge coefficients for the traditional tide gates ranged between 0.12 and 0.86. An average discharge coefficient value of 0.38 was recommended. At US 101 Slough head loss coefficients were separated into three categories based on opening phase (opening, fully open, and closing phases). of the gate. Gate 1 showed that the average head loss coefficient value of each phase decreased between the opening, fully open and closing phases. Gate 2 did not have any measurements taken during its closing phase since the closing occurred suddenly. However, its opening phase also had a higher average head loss coefficient than the fully open phase. Gate 2 additionally had smaller gate opening

angles than Gate 1 that resulted in faster velocities through the gate opening and overall smaller head loss coefficients. A head loss coefficient of 5.26 was recommended for modeling because it was the average value of both gates fully open phase. The opening phase was excluded from the average because the gates opened fairly quickly and were only a small portion of the total opening. The closing phases were also excluded due to the differences between how each gate closed (i.e., Gate 1 slowly closed while Gate 2 suddenly closed). Further investigation into various flows and additional angle measurements at both sites could result in a further understanding of how the coefficients change throughout the gate openings.

REFERENCES

- Brunner, G.W. (2012). “HEC-RAS, River Analysis System Hydraulic Reference Manual.” *US Army Corps of Engineers: Hydraulic Engineering Center*.
- Burrows, R., and J. Emmonds. (1988). “Energy head implications of the installation of circular flap gates on drainage outfalls.” *J. Hydraulic Research* 26(2): 131–142.
- California Department of Fish and Game (CDFG). (2004). *Appendix IX-A: Culvert Criteria for Fish Passage*. California Salmonid Stream Habitat Restoration Manual.
- California Department of Fish and Wildlife (CDFW). (2020). Passage Assessment Database (PAD) Query Tool, <https://nrm.dfg.ca.gov/PAD/Default.aspx> (accessed 10 April 2020).
- CalFish, (2018). Standards, <<https://www.calfish.org/Resources/Standards.aspx>> (accessed 13 December 2020).
- Cassan, L., Guiot, L., and Belaud, G. (2018). “Modeling of Tide Gate to Improve Fish Passability.” *7th IAHR International Symposium on Hydraulic Structures*. Aachen, Germany.
- CTC & Associates (2016). *Tide Gates: Technical and Ecological Considerations*. Caltrans Division of Research, Innovation and System Information (DRISI).
- Dahl, T.E. and Allord, G.J. (1997). *Technical Aspects of Wetlands: History of Wetlands in the Conterminous United States*, United States Geological Survey <<https://water.usgs.gov/nwsum/WSP2425/history.html>> (accessed 22 July 2020).
- Giannico, G., and Souder, J. A. (2005). “Tide Gates in the Pacific Northwest.” *Oregon State University*, 33.
- Greene, C., Hall, J., Beamer, E., Henderson, R. and Brown, B. (2012). *Biological and Physical Effects of “Fish-Friendly” Tide Gates*. Estuary and Salmon Restoration Program, Washington.
- Guiot, L., Cassan, L. and Belaud, G. (2020). “Modeling the Hydromechanical Solution for Maintaining Fish Migration Continuity at Coastal Structures.” *J. Irrig. Drain Eng.* 146(12).

- Humboldt State University (HSU) and Michael Love and Associates, Inc. (2020). *Eureka-Arcata Corridor Tide Gate Replacement Project: Pre-Project Baseline Monitoring: Final Report*. Caltrans District 1.
- Keaton, J.N. (2004). *Simulating Flooding Effects of Proposed Water-Control Structures for Lake Tecumseh and Adjacent Wetlands in Virginia Beach, Virginia*. United States Geological Survey and U.S. Fish and Wildlife Service.
- Lang, P., Desombre, J., Ata, R., Goeury, C., and Hervouet, J.M. (2014) “Telemac Modelling System: TELEMAC-2D Software User Manual.” *Research and Development Directorate of French Electricity Board (EDF-R&D)*.
- Love, M., Shea, R., Allen, S. and James, T. (2013). *Martin Slough Enhancement Project, Eureka CA Basis of Design Report*. Redwood Community Action Agency, Eureka, CA.
- Moyle, P.B., Lusardi, R.A., Samuel, P.J. and Katz, J.V.E. (2017). *State of Salmonids: Status of California's Emblematic Fishes*. Center of Watershed Sciences, University of California, Davis and California Trout.
- National Marine Fisheries Service (NMFS). (2001). *Guidelines for Salmonid Passage at Stream Crossings*. National Marine Fisheries Service Southwest Region.
- Novak, S. J. and Goodell, C.R. (2006). “Using HEC--RAS 3.1.3 to Model and Design Tide Gate Systems.” *Proceedings of the West Coast Symposium on the Effects of Tide Gates on Estuarine Habitats and Fishes*, 2006.
- Replogle, J.A. and Wahlin, B.T. (2003). “Head Loss Characteristics of Flap Gates at the Ends of Drain Pipes.” *American Society of Agricultural Engineers*, 46(4), 1077-1084.
- Rossman, L.A., (2015). “Storm Water Management Model User's Manual Version 5.1.” *National Risk Management Research Laboratory: U.S. Environmental Protection Agency*
- Schall, J.D., Thompson, P.L., Zerges, S.M., Kilgore, R.T. and Morris, J.L. (2012). *Hydraulic Design of Highway Culverts*, 3rd Ed., Federal Highway Administration, Washington D.C.
- Stahl, T. (2006). “Oregon's Fish-passage Requirements for Tide Gates.” *Proceedings of the West Coast Symposium on the Effects of Tide Gates on Estuarine Habitats and Fishes*, 2006.

- Tonnes, D. M. (2006). "Fish Use and Water Quality in Select Channels Regulated by Tide Gates within the Snohomish River Estuary." Technical Assessment, National Marine Fisheries Service.
- United States Department of Agriculture (USDA). (1971). *Section 16 Drainage of Agricultural Land*. U.S. Department of Agriculture, Soil Conservation Service, Washington D.C.
<<https://directives.sc.egov.usda.gov/OpenNonWebContent.aspx?content=18370.wba>> (accessed 15 April 2020).
- U.S. Fish and Wildlife Service (USFWS). (2005). *Recovery Plan for the Tidewater Goby (Eucyclogobius newberryi)*. U.S. Fish and Wildlife Service, Portland, Oregon. vi + 199 pp.
- U.S. Fish and Wildlife Service (USFWS). (2013a). *Recovery Plan for Tidal Marsh Ecosystems of Northern and Central California*. Pacific Southwest Region, Region 8 U.S. Fish and Wildlife Service, Sacramento.
- U.S. Fish and Wildlife Service (USFWS). (2013b). Humboldt Bay Fish,
<https://www.fws.gov/refuge/Humboldt_Bay/wildlife_and_habitat/HumboldtFish1.html> (accessed 15 April 2020).
- U.S. Geological Survey (USGS). (1997). *National Water Summary on Wetland Resources*. United States Geological Survey Water Supply Paper 2425.
<https://water.usgs.gov/nwsum/WSP2425/state_highlights_summary.html> (accessed 7 October 2020)

APPENDICES

*Appendix A: Raw ADCP Discharge, Velocity and Angle Measurements**Table A 1. Discharge, velocity, and gate angle opening for Gannon Slough Gate 1.*

Date/Time	Discharge (cfs)	Velocity through Gate (fps)	Gate Angle Opening (degrees)
05/18/20 11:31	2.769	10.87	0.3
05/18/20 11:41	4.735	2.67	2.1
05/18/20 11:46	3.498	1.44	2.9
05/18/20 11:55	4.647	1.70	3.3
05/18/20 12:04	5.269	1.95	3.3
05/18/20 12:12	6.533	2.45	3.3
05/18/20 12:42	8.401	3.79	2.9
05/18/20 12:55	5.530	2.58	2.9
05/18/20 13:04	4.528	2.34	2.7
05/18/20 13:15	2.092	1.17	2.6
05/18/20 13:30	4.140	3.60	1.8
05/18/20 13:52	3.549	11.88	0.5

Table A 2. Discharge, velocity, and gate angle opening for Gannon Slough Gate 2.

Date/Time	Discharge (cfs)	Velocity through Gate (fps)	Gate Angle Opening (degrees)
05/18/20 11:41	7.526	2.70	3.3
05/18/20 11:46	8.786	2.18	4.8
05/18/20 11:55	10.754	2.23	5.8
05/18/20 12:04	9.580	1.88	6.2
05/18/20 12:12	9.561	2.00	5.9
05/18/20 12:26	11.221	2.25	6.3
05/18/20 12:42	11.257	2.53	5.8
05/18/20 12:55	10.362	2.26	6.2
05/18/20 13:04	11.331	2.54	6.2
05/18/20 13:15	11.149	3.06	5.3
05/18/20 13:30	8.398	3.28	4.0
05/18/20 14:06	2.486	14.32	0.3
05/18/20 14:22	1.257	3.19	0.7

Table A 3. Discharge, velocity, and gate angle opening for Gannon Slough Gate 3.

Date/Time	Discharge (cfs)	Velocity through Gate (fps)	Gate Angle Opening (degrees)
05/18/20 11:31	6.953	7.44	1.1
05/18/20 11:41	13.557	5.54	2.9
05/18/20 11:46	15.896	5.12	3.7
05/18/20 11:55	21.159	5.42	4.7
05/18/20 12:04	19.060	4.95	4.7
05/18/20 12:12	17.442	4.80	4.5
05/18/20 12:26	16.141	4.98	4.1
05/18/20 12:42	11.909	5.19	3.0
05/18/20 12:55	12.284	5.04	3.3
05/18/20 13:04	11.218	5.39	2.9
05/18/20 13:15	11.746	6.34	2.7
05/18/20 13:30	6.277	5.46	1.8

Table A 4. Discharge, velocity, and gate angle opening for US 101 Slough Gate 1.

Date/Time	Discharge (cfs)	Velocity through Gate (fps)	Gate Angle Opening (degrees)
6/10/20 7:16	6.2	0.65	34.61
6/10/20 7:19	8.5	0.62	46.67
6/10/20 7:23	9.1	0.53	55.77
6/10/20 7:28	13.1	0.71	59.83
6/10/20 7:31	15.2	0.74	66.04
6/10/20 7:36	18.2	0.89	67.30
6/10/20 7:41	22.4	1.11	68.51
6/10/20 7:45	19.8	1.05	67.63
6/10/20 8:58	7.5	1.07	57.99
6/10/20 9:01	7.9	1.22	55.41
6/10/20 9:04	8.3	1.37	54.27
6/10/20 9:07	7.9	1.36	54.07
6/10/20 9:12	7.8	1.39	54.07
6/10/20 9:20	7.2	1.42	52.00
6/10/20 9:25	7.8	1.66	49.72
6/10/20 9:33	5.8	1.35	48.49
6/10/20 9:38	6.2	1.50	46.40
6/10/20 9:47	7.8	1.97	41.99
6/10/20 9:52	4.6	1.13	39.69
6/10/20 9:56	5.9	1.74	32.62
6/10/20 9:59	4.9	1.48	30.54
6/10/20 10:03	4.8	1.49	28.81
6/10/20 10:07	3.5	1.13	26.57
6/10/20 10:13	4.3	1.36	26.10
6/10/20 10:17	3.8	1.20	25.64
6/10/20 10:22	4.0	1.26	24.70
6/10/20 10:41	1.8	0.56	21.31

Table A 5. Discharge, velocity, and gate angle opening for US 101 Slough Gate 2.

Date/Time	Discharge (cfs)	Velocity through Gate (fps)	Gate Angle Opening (degrees)
6/10/20 7:14	3.9	0.67	20.30
6/10/20 7:18	8.0	0.78	36.87
6/10/20 7:22	9.3	0.77	42.92
6/10/20 7:26	11.5	0.84	48.24
6/10/20 7:29	13.4	0.83	55.03
6/10/20 7:34	15.9	0.98	57.00
6/10/20 7:38	21.2	1.33	58.15
6/10/20 7:43	21.5	1.41	58.15
6/10/20 8:57	7.3	1.04	58.15

Appendix B: Component Head Loss and Discharge Coefficient Calculations for Gannon Slough

Table B 1. Upstream and culvert water depths, component head loss values for entrance and friction loss, and discharge coefficients for Gannon Slough Gate 1.

Date/Time	STA 1.25 Water Level (ft)	STA 1.75 Water Level (ft)	Entrance Loss (ft)	Friction Loss (ft)	Discharge Coefficient
05/18/20 11:31	2.49	4.38	0.004	0.00005	0.859
05/18/20 11:41	2.41	4.31	0.005	0.00016	0.215
05/18/20 11:46	2.36	4.26	0.004	0.00009	0.116
05/18/20 11:55	2.26	4.16	0.011	0.00019	0.141
05/18/20 12:04	2.14	4.04	0.008	0.00028	0.166
05/18/20 12:12	2.04	3.94	0.011	0.00049	0.214
05/18/20 12:42	1.65	3.54	0.000	0.00148	0.368
05/18/20 12:55	1.43	3.33	0.010	0.00096	0.269
05/18/20 13:04	1.27	3.18	0.017	0.00090	0.258
05/18/20 13:15	1.04	2.96	0.036	0.00035	0.144
05/18/20 13:30	0.71	2.67	0.066	0.00437	0.533
05/18/20 13:52	0.44	2.35	0.015	0.01392	2.223

Table B 2. Upstream and culvert water depths, component head loss values for entrance and friction loss, and discharge coefficients for Gannon Slough Gate 2.

Date/Time	STA 1.25 Water Level (ft)	STA 1.75 Water Level (ft)	Entrance Loss (ft)	Friction Loss (ft)	Discharge Coefficient
05/18/20 11:41	2.41	4.31	0.005	0.00016	0.217
05/18/20 11:46	2.36	4.26	0.004	0.00009	0.177
05/18/20 11:55	2.26	4.16	0.011	0.00019	0.185
05/18/20 12:04	2.14	4.04	0.008	0.00028	0.161
05/18/20 12:12	2.04	3.94	0.011	0.00049	0.175
05/18/20 12:26	1.87	3.76	0.006	0.00087	0.205
05/18/20 12:42	1.65	3.54	0.000	0.00148	0.246
05/18/20 12:55	1.43	3.33	0.010	0.00096	0.235
05/18/20 13:04	1.27	3.18	0.017	0.00090	0.280
05/18/20 13:15	1.04	2.96	0.036	0.00035	0.375
05/18/20 13:30	0.71	2.67	0.066	0.00437	0.486

Table B 3. Upstream and culvert water depths, component head loss values for entrance and friction loss, and discharge coefficients for Gannon Slough Gate 3.

Date/Time	STA 1.25 Water Level (ft)	STA 1.75 Water Level (ft)	Entrance Loss (ft)	Friction Loss (ft)	Discharge Coefficient
05/18/20 11:31	2.49	4.38	0.004	0.0000506	0.588
05/18/20 11:41	2.41	4.31	0.005	0.0001609	0.445
05/18/20 11:46	2.36	4.26	0.004	0.0000926	0.415
05/18/20 11:55	2.26	4.16	0.011	0.0001859	0.450
05/18/20 12:04	2.14	4.04	0.008	0.0002769	0.422
05/18/20 12:12	2.04	3.94	0.011	0.0004885	0.419
05/18/20 12:26	1.87	3.76	0.006	0.0008745	0.455
05/18/20 12:42	1.65	3.54	0.000	0.0014750	0.505
05/18/20 12:55	1.43	3.33	0.010	0.0009585	0.526
05/18/20 13:04	1.27	3.18	0.017	0.0009025	0.595
05/18/20 13:15	1.04	2.96	0.036	0.0003536	0.776
05/18/20 13:30	0.71	2.67	0.066	0.0043747	0.808

Appendix C: Component Head Loss Calculations for US 101 Slough

Table C 1. Head loss components for US 101 Slough Gate 1.

Date/Time	Total Head Loss (ft)	Entrance Head Loss (ft)	Trash Rack Head Loss (ft)	Friction Head Loss (ft)	Tide Gate Head Loss (ft)
6/10/2020 7:16	0.098	0.00032	0.029	0.00016	0.069
6/10/2020 7:19	0.111	0.00064	0.041	0.00032	0.069
6/10/2020 7:23	0.141	0.00079	0.069	0.00040	0.071
6/10/2020 7:28	0.170	0.00177	0.095	0.00093	0.073
6/10/2020 7:31	0.187	0.00252	0.107	0.00134	0.077
6/10/2020 7:36	0.204	0.00398	0.118	0.00217	0.082
6/10/2020 7:41	0.221	0.00658	0.133	0.00371	0.081
6/10/2020 7:45	0.236	0.00560	0.147	0.00324	0.083
6/10/2020 8:58	0.321	0.00432	0.255	0.00499	0.062
6/10/2020 9:01	0.332	0.00506	0.263	0.00598	0.064
6/10/2020 9:04	0.339	0.00592	0.265	0.00720	0.068
6/10/2020 9:07	0.342	0.00585	0.281	0.00740	0.055
6/10/2020 9:12	0.354	0.00610	0.283	0.00797	0.065
6/10/2020 9:20	0.368	0.00589	0.291	0.00815	0.071
6/10/2020 9:25	0.358	0.00719	0.290	0.01015	0.061
6/10/2020 9:33	0.375	0.00442	0.303	0.00655	0.068
6/10/2020 9:38	0.351	0.00473	0.269	0.00686	0.077
6/10/2020 9:47	0.232	0.00576	0.160	0.00727	0.066
6/10/2020 9:52	0.210	0.00167	0.118	0.00195	0.090
6/10/2020 9:56	0.154	0.00242	0.077	0.00264	0.075
6/10/2020 9:59	0.145	0.00150	0.062	0.00156	0.082
6/10/2020 10:03	0.126	0.00131	0.060	0.00131	0.065
6/10/2020 10:07	0.118	0.00064	0.044	0.00062	0.073
6/10/2020 10:13	0.114	0.00089	0.039	0.00082	0.074
6/10/2020 10:17	0.121	0.00067	0.048	0.00061	0.072
6/10/2020 10:22	0.111	0.00069	0.041	0.00061	0.069
6/10/2020 10:41	0.081	0.00010	0.019	0.00008	0.062

Table C 2. Head loss components for US 101 Slough Gate 2.

Date/Time	Total Head Loss (ft)	Entrance Head Loss (ft)	Trash Rack Head Loss (ft)	Friction Head Loss (ft)	Tide Gate Head Loss (ft)
6/10/2020 7:14	0.096	0.00013	0.023	0.00006	0.073
6/10/2020 7:18	0.105	0.00056	0.041	0.00028	0.063
6/10/2020 7:22	0.137	0.00080	0.061	0.00040	0.075
6/10/2020 7:26	0.156	0.00132	0.082	0.00068	0.073
6/10/2020 7:29	0.180	0.00189	0.102	0.00099	0.076
6/10/2020 7:34	0.204	0.00293	0.112	0.00158	0.089
6/10/2020 7:38	0.207	0.00564	0.127	0.00313	0.074
6/10/2020 7:43	0.226	0.00638	0.143	0.00365	0.077
6/10/2020 8:57	0.331	0.00404	0.254	0.00458	0.073